# Material Characterization and Determination of MEPDG Input Parameters for Indiana Superpave 5 Asphalt Mixtures

**Seonghwan Cho, Tandra Bagchi, Jongmyung Jeon, John E. Haddock**

## AUTHORS

**Seonghwan Cho, PhD**
Pavement Research Engineer
Indiana Department of Transportation

**Tandra Bagchi**
Graduate Research Assistant
Lyles School of Civil Engineering
Purdue University

**Jongmyung Jeon, PhD**
Research Associate
Lyles School of Civil Engineering
Purdue University

**John E. Haddock, PhD, PE**
Professor of Civil Engineering
Director of the Local Technical Assistance Program
Purdue University
(765) 496-3996
jhaddock@purdue.edu
*Corresponding Author*

## JOINT TRANSPORTATION RESEARCH PROGRAM

The Joint Transportation Research Program serves as a vehicle for INDOT collaboration with higher education institutions and industry in Indiana to facilitate innovation that results in continuous improvement in the planning, design, construction, operation, management and economic efficiency of the Indiana transportation infrastructure. https://engineering.purdue.edu/JTRP/index_html

Published reports of the Joint Transportation Research Program are available at http://docs.lib.purdue.edu/jtrp/.

# TECHNICAL REPORT DOCUMENTATION PAGE

| 1. Report No.<br>FHWA/IN/JTRP-2024/06 | 2. Government Accession No. | 3. Recipient's Catalog No. |
|---|---|---|
| **4. Title and Subtitle**<br>Material Characterization and Determination of MEPDG Input Parameters for Indiana Superpave 5 Asphalt Mixtures | | **5. Report Date**<br>March 2024 |
| | | **6. Performing Organization Code** |
| **7. Author(s)**<br>Seonghwan Cho, Tandra Bagchi, Jongmyung Jeon, and John E. Haddock | | **8. Performing Organization Report No.**<br>FHWA/IN/JTRP-2024/06 |
| **9. Performing Organization Name and Address**<br>Joint Transportation Research Program<br>Hall for Discovery and Learning Research (DLR), Suite 204<br>207 S. Martin Jischke Drive<br>West Lafayette, IN 47907 | | **10. Work Unit No.** |
| | | **11. Contract or Grant No.**<br>SPR-4514 |
| **12. Sponsoring Agency Name and Address**<br>Indiana Department of Transportation (SPR)<br>State Office Building<br>100 North Senate Avenue<br>Indianapolis, IN 46204 | | **13. Type of Report and Period Covered**<br>Final Report |
| | | **14. Sponsoring Agency Code** |

**15. Supplementary Notes**

Conducted in cooperation with the U.S. Department of Transportation, Federal Highway Administration.

**16. Abstract**

   Superpave 5 (SP 5) has the ability to slow asphalt binder aging in asphalt pavements, which is why the SP 5 mix with optimum asphalt binder content to yield 5% air voids has recently been used in Indiana roads. INDOT also uses the AASHTOWare Pavement ME design software in pavement design, and the current asphalt aging prediction model in Pavement ME was developed based on the conventional Superpave asphalt mixture (design air voids 4%) design method. For the successful use of the SP 5 mixture design method with Pavement ME, the input level and input parameters play a significant role.

   The objective of this study was to determine pavement performance using the three different input levels (Level 1, 2, and 3) and to recommend the necessary Pavement ME input parameters for SP 5 mixtures for accurate pavement performance prediction. The results show that Levels 2 and 3 are underpredicting or overpredicting the pavements' distresses. Therefore, to capture the benefit of SP 5 pavement design, the Level 1 inputs (lab test results) were recommended for the Pavement ME. The findings of this research will provide guidance on using accurate input parameters for the Pavement ME design for SP 5 mixtures, resulting in more accurate asphalt pavement performance predictions during the pavement design process. It is anticipated that this will result in longer asphalt pavement service lives, which is a cost-effective benefit for INDOT.

| **17. Key Words**<br>asphalt mixture, Superpave 5, input level, Pavement ME, pavement performance | | **18. Distribution Statement**<br>No restrictions. This document is available through the National Technical Information Service, Springfield, VA 22161. | |
|---|---|---|---|
| **19. Security Classif. (of this report)**<br>Unclassified | **20. Security Classif. (of this page)**<br>Unclassified | **21. No. of Pages**<br>55 including appendices | **22. Price** |

Form DOT F 1700.7 (8-72)                                    Reproduction of completed page authorized

# EXECUTIVE SUMMARY

## Introduction

The stiffness of asphalt materials increases over the pavement service life as a result of the oxidation process. This phenomenon, commonly known as aging, results in asphalt binder embrittlement and thus a decrease in asphalt mixture resistance to cracking. One of the most important benefits of using Superpave 5 (SP 5) asphalt mixtures is their ability to slow asphalt binder aging in asphalt pavements (Huber et al., 2019). The researchers of this study compared the 5-year binder aging levels and asphalt mixture cracking and rutting performance of SP 5 and conventional Superpave asphalt mixture (SP 4) constructed in a 2013 trial project (Huber et al., 2019). Additionally, visual field inspection revealed the SP 5 asphalt mixture had better cracking and rutting performance than the SP 4 asphalt mixture (Huber et al., 2019). In order to relate asphalt mixture properties to asphalt pavement design, it is necessary during the pavement design process to predict anticipated in-service asphalt pavement performance-based laboratory asphalt mixture properties and expected traffic level and climate conditions.

INDOT uses the AASHTOWare Pavement ME Design software for pavement design. AASHTO's Pavement ME Design software implements the new mechanistic-empirical pavement design and analysis method. Agencies adopting Pavement ME Design require appropriate input values corresponding to local material specifications, traffic loading, and environmental conditions. Based on the quality of the input data, there are three levels (Levels 1 to 3) of local materials data that can be used in the Pavement ME program (Esfandiarpour et al., 2013). To ensure good prediction results, the embedded Pavement ME models must be properly calibrated to account for INDOT materials. However, the current asphalt aging prediction model in Pavement ME was developed based on the conventional Superpave asphalt mixture (SP 4) design method, which assumes an in-place air void content of 7%. However, the Global Aging Model (GAS model) may not be properly calibrated for air voids lower than 6%. Also, the GAS model does not accurately capture the effects of air voids on aging. So, the long-term pavement performance of the SP 5 mixture cannot be determined by using the current aging model of Pavement ME. The viscoelastic parameters (dynamic modulus and phase angle) are the most important factors in the current aging prediction model. In order to successfully use the Superpave 5 asphalt mixture design method with Pavement ME, updated asphalt aging prediction models must be determined for both Levels 1 and 2 Pavement ME designs and the input level and input parameters play a significant role. So, it is necessary to determine the pavement performance using the three different input levels (Level 1, 2, and 3) and different aging conditions and to recommend the necessary Pavement ME input parameters for SP 5 asphalt mixtures for the prediction of long-term accurate pavement performance. Additionally, the anticipated performance of SP 5 asphalt mixtures, as compared to SP 4 mixtures will be evaluated using the Pavement ME software.

The primary objective of the proposed study was to evaluate the accuracy of Pavement ME to predict the pavement performance of the SP 5 mixture, and also to determine the necessary Pavement ME input parameters for Superpave 5 asphalt mixtures. Additionally, the anticipated performance of Superpave 5 asphalt mixtures were compared to conventional Superpave mixtures to better characterize the possible long-term performance enhancements of using Superpave 5 asphalt mixtures.

## Findings

Pavement ME simulations have shown that there is a significant difference between Level 1, Level 2, and Level 3 thermal cracking, rutting, bottom-up fatigue cracking, and top-down fatigue cracking. Levels 2 and 3 underestimated the benefits of SP 5 due to the use of default values calibrated based on SP 4, while Level 1 might capture the benefits of SP 5 using lab test results. Also, SP 4 mixtures indicated greater permanent deformation than SP 5 mixtures due to higher air voids and consolidation effect under the traffic loading. And SP 5 mixtures showed better resistance against cracking performance based on the Pavement-ME simulation results due to higher in-place density and lower oxidative aging. So, to capture the benefit of SP 5 pavement design, the Level 1 inputs (lab test results) are recommended for the Pavement ME.

## Implementation

To determine the representative Superpave 5 input parameters for Pavement ME and evaluate the performance of Superpave 5 mixtures in comparison to conventional Superpave mixtures, the viscoelastic parameters, cracking, and rutting behavior of asphalt mixtures designed by both Superpave 5 and the conventional Superpave design methods were compared at two aging levels, both short- and long-term. Using Pavement ME, performance predictions for all the mixtures were conducted and compared between the mixtures and field performance of the Superpave 5 and the conventional Superpave.

In this study, 5 days aging at 85°C for short-term and 12 days aging at 85°C for long-term was selected. Laboratory tests were divided into mixture testing and binder testing. For the mixture test, dynamic modulus, cyclic fatigue test, and Hamburg Wheel Tracking Test (HWTT) were conducted. For the binder test, Dynamic Shear Modulus (DSR), frequency sweep test, and Fourier Transform Infrared Spectroscopy (FTIR) tests were conducted. The dynamic modulus test results along with DSR test results were used as input for Pavement ME simulations.

CONTENTS

# LIST OF TABLES

# LIST OF FIGURES

# 1. PROJECT OVERVIEW

## 1.1 Introduction

Conventional Superpave design requires compaction of asphalt mixture at 4% air voids in the laboratory and satisfying all AASHTO M323 limits (AASHTO, 2013). The mixture is then placed at 7% air voids in the field with the assumption that it will be compacted to the design air void content by the traffic (Huber et al., 2019; Yan et al., 2022). However, many of the mixtures do not reach the target air void several years into service (Watson et al., 2005). In this study, the conventional Superpave mix is denoted as SP 4.

Modification of the Superpave asphalt mixture design can achieve in-place density which can enhance asphalt mixture's durability and pavement life (Haddock et al., 2020). To achieve this, the design air void content is kept at 5% and the modification in aggregate gradation is performed without lowering the effective binder content (Ali, 2019; Haddock et al., 2020, Hekmatfar et al., 2015, Yan et al., 2022). Increasing the average in-place asphalt mixture densities to 95% would significantly decrease asphalt binder aging which could achieve a 12% to 20% increase in pavement life (Hekmatfar et al., 2015). This special mix, which was developed by Laboratoire Centrale des Ponts et Chaussees (LCPC) in France in the 1970s, specifies the same air void content for both design and construction (Moutier, 1982), and the new mix design is referred to as Superpave 5 (SP 5).

In July 2013, the first trial section of Superpave 5 in Indiana was placed as the party of an existing project (Huber et al., 2019). After successful laboratory testing of the Superpave 5 asphalt mixture design method, two controlled field tests (Hekmatfar et al., 2015), and one full-scale demonstration project (Montoya et al., 2018), the Indiana Department of Transportation (INDOT) developed a provisional Superpave 5 specification and established 12 additional projects based on the provisional specification. These projects were uncontrolled, meaning that INDOT did not help with the mixture design or mixture production placement, with the goal of allowing contractors to use their expertise to meet the specification and to determine if any additional adjustments were needed to the Superpave 5 asphalt mixture design method (Haddock et al., 2020). The SP 5 mixture was successfully constructed without any issues. As a result, the Superpave 5 asphalt mixture design method has become the default asphalt mixture design method for INDOT.

The stiffness of asphalt materials increases over the pavement service life as a result of the oxidation process. This phenomenon, commonly known as aging, results in asphalt binder embrittlement and thus a decrease in asphalt mixture resistance to cracking. One of the most important benefits of using SP 5 asphalt mixtures is their ability to slow asphalt binder aging in asphalt pavements (Huber et al., 2019). The researchers compared the 5-year binder aging levels and asphalt mixture cracking and rutting performance of SP 5 and SP 4 asphalt mixtures constructed in a 2013 trial project (Huber et al., 2019). Additionally, visual field inspection revealed the SP 5 asphalt mixture had better cracking and rutting performance than did the SP 4 asphalt mixture (Huber et al., 2019). In order to relate asphalt mixture properties to asphalt pavement design, it is necessary during the pavement design process, to predict anticipated in-service asphalt pavement performance-based laboratory asphalt mixture properties and expected traffic level and climate conditions.

INDOT uses the AASHTOWare Pavement ME Design software for pavement design. AASHTO Pavement ME Design software implements the new mechanistic-empirical pavement design and analysis method. Agencies adopting Pavement ME Design require appropriate input values corresponding to local material specifications, traffic loading, and environmental conditions. Based on the quality of the input data, there are three levels (Levels 1 to 3) of local materials data that can be used in the Pavement ME program (Esfandiarpour et al., 2013). However, to ensure good prediction results, the embedded Pavement ME models must be properly calibrated to account for INDOT materials. However, the current asphalt aging prediction model in Pavement ME was developed based on the conventional Superpave asphalt mixture (SP 4) design method, which assumes design air voids content of 4%. In order to successfully use the Superpave 5 asphalt mixture design method with Pavement ME, updated asphalt aging prediction models must be determined for both Levels 1 and 2 Pavement ME designs.

In order to successfully use the SP 5 asphalt mixture design method with Pavement ME, the input level along with input parameters play a significant role. So, it is necessary to determine the pavement performance using the three different input levels (Levels 1, 2, and 3) and different aging conditions and to recommend the necessary Pavement ME input parameters for SP 5 asphalt mixtures for the prediction of accurate pavement performance in the long term. Additionally, the anticipated performance of SP 5 asphalt mixtures, as compared to SP 4 mixtures will be evaluated using the Pavement ME software.

The findings of this research will provide guidance to INDOT by modifying the Pavement ME aging prediction model for Superpave 5-designed mixtures, resulting in a more accurate asphalt pavement performance predictions during the pavement design process. It is anticipated that incorporating the lower aging levels resulting from the use of Superpave 5-designed mixtures in the pavement design process will result in longer predicted asphalt pavement service lives and a cost-effective benefit for INDOT.

## 1.2 Objectives

The primary objective of the proposed study is to evaluate the accuracy of Pavement ME to predict the pavement performance of the SP 5 mixture. Also, to determine the necessary Pavement ME input parameters for

Superpave 5 asphalt mixtures. Additionally, the anticipated performance of Superpave 5 asphalt mixtures, as compared to conventional Superpave mixtures will be evaluated using the software, to better characterize the possible long-term performance enhancements of using Superpave 5 asphalt mixtures.

## 2. LITERATURE REVIEW AND SENSITIVITY ANALYSIS

### 2.1 Benefits of Superpave 5 Mixture

The stiffness of asphalt materials increases over the pavement service life as a result of the oxidation process. This phenomenon, commonly known as aging, results in asphalt binder embrittlement and thus a decrease in asphalt mixture resistance to cracking. One of the most important benefits of using Superpave 5-designed asphalt mixtures is their ability to slow asphalt binder aging in asphalt pavements. This benefit was demonstrated by Huber et al. (2019). Their study compared the 5-year binder aging levels and asphalt mixture cracking and rutting performance of Superpave 5, and conventional Superpave asphalt mixtures constructed in a 2013 trial project. The binder performance grades of extracted and recovered binders from the two test sections showed lower binder aging in the Superpave 5 asphalt mixtures. Additionally, visual field inspection revealed the Superpave 5 asphalt mixture had better cracking and rutting performance than did the conventional Superpave asphalt mixture.

### 2.2 Limitations of Pavement ME for Aging Model of Superpave 5 Mixture

In order to relate asphalt mixture properties to asphalt pavement design, it is necessary during the pavement design process, to predict anticipated in-service asphalt pavement performance-based laboratory asphalt mixture properties and expected traffic level and climate conditions. INDOT does this using the AASHTOWare Pavement ME Design software. However, to ensure good prediction results, the embedded Pavement ME models must be properly calibrated to account for INDOT materials. However, the current asphalt aging prediction model in Pavement ME was developed based on the conventional Superpave asphalt mixture (SP 4) design method, which assumes an in-place air void content of 7%. However, the Global Aging Model (GAS model) may not be properly calibrated for air voids lower than 6%. Also, the GAS model does not accurately capture the effects of air voids on the aging. So, the long-term pavement performance of the SP 5 mixture cannot be determined by using the current aging model of Pavement ME. The viscoelastic parameters (dynamic modulus and phase angle) are the most important factors in the current aging prediction model. In order to successfully use the Superpave 5 asphalt mixture design method with Pavement ME, updated asphalt aging prediction models must be determined for both Levels 1 and 2 Pavement ME designs.

### 2.3 Research Approach and Finalize Test Plan

To fulfill the main study objective of determining the representative Superpave 5 input parameters for Pavement ME and additionally evaluate the performance of Superpave 5 mixtures in comparison to conventional Superpave mixtures, the viscoelastic parameters, cracking, and rutting behavior of asphalt mixtures designed by both Superpave 5, and the conventional Superpave design methods will be compared at two aging level, short- and long-term. Using Pavement ME, performance predictions for all the mixtures will be conducted and compared, both between the Superpave 5 and conventional Superpave mixtures, as well as with the field performance.

In this study, 5 days aging at 85°C for short-term and 12 days aging at 85°C for long-term was selected. Laboratory tests are divided into mixture testing and binder testing. For the mixture test, dynamic modulus, cyclic fatigue test, and Hamburg Wheel Tracking Test (HWTT) were conducted and for the binder test, Dynamic Shear Modulus (DSR), frequency sweep test, and Fourier Transform Infrared Spectroscopy (FTIR) test were conducted. The dynamic modulus test results along with DSR test results were used as input for Pavement ME simulations. The flow chart in Figure 2.1 shows the details of the laboratory tests that were conducted in this study.
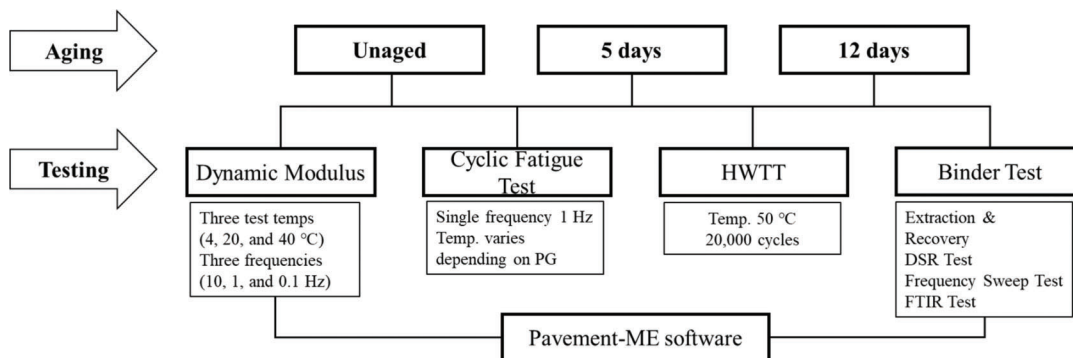


**Figure 2.1**   Laboratory test plan.

# 3. SAMPLE PREPARATION AND LABORATORY CONDITIONING

## 3.1 Sample Collection

### 3.1.1 Plant Mix SP 5 Sample

The SP 5 mixtures were collected from three plants operated by different contractors: Milestone (MS), Rieth Riley (RR), and E&B (EB). Four different mixture types and three distinct Performance Grades (PG) were considered for this project, aligning with typical pavement design practices in Indiana. A total of eleven mixtures were gathered for laboratory testing. Table 3.1 illustrates the volumetric properties and mix design information of the collected SP 5 mixtures.

The conventional SP 4 mixtures were also collected. Two mixture types, both having the same PG 64-22, were chosen for a comparative study with SP 5 mixtures. Table 3.2 presents the mix design information for the collected SP 4 mixtures.

### 3.1.2 Field Core Sample

Field cores were also collected from three distinct SP 5 projects. Table 3.3 presents information on the selected projects, all of which were constructed in 2018. The mix for US 231 utilized a PG 70-22 binder, while the mixes for US 30 and US 31 employed a PG 76-22 binder. Ten cores were sampled from each project. These collected cores underwent both binder testing and mixture performance testing. Subsequently, the test results were compared with those of specimens prepared at various aging levels in the laboratory.

## 3.2 Aging Process of the Collected Sample

### 3.2.1 Selection of Mix Types for Aging Effect Study

The most significant benefit of the SP 5 mix is its ability to decelerate the initial aging of the pavement by increasing in-place density. The in-place air voids of the conventional SP 4 mix are 7%, whereas, for SP 5, it is reduced to 5%. This difference in air voids between the two mixtures can influence pavement aging. To assess the difference in aging effects between SP 5 and SP 4 and to validate the aging effect of SP 5 in Pavement-ME, two mixtures each for SP 5 and SP 4 were chosen. Two mixtures of SP 4 in Table 3.2 and MS1 and RR1 in Table 3.1 which match two SP 4 mixes were selected. EB4 (PG76-22) was also selected to evaluate the aging effect according to binder grades.

### 3.2.2 Aging Process

Mixture conditioning in the laboratory is conducted to simulate field conditions and provide a more accurate prediction of the properties and performance of Hot Mix Asphalt (HMA). According to Zhang et al. (2020), 5 days of aging in the laboratory can simulate approximately 8 years of field aging, and 12 days of aging can simulate around 20 years of field aging. Consequently, three aging levels—unaged, 5 days of

TABLE 3.1
**Mix design information of collected SP 5 mixtures**

| Mix ID | NMAS (mm) | PG | $P_b$ | $P_{be}$ | % RAP (ABR) | $N_{des}$ | VMA | VFA | TSR |
|--------|-----------|-------|-------|----------|-------------|-----------|------|------|------|
| MS1 | 9.5 | 64-22 | 6.4 | 4.9 | 23.2 | 30 | 16.5 | 69.7 | 94.5 |
| MS4 | | 70-22 | 6.3 | 5.1 | 23.6 | 50 | 17.2 | 70.9 | 89.2 |
| EB1 | | 70-22 | 6.7 | 5.2 | 18.5 | 50 | 16.8 | 70.2 | 85.0 |
| EB4 | | 76-22 | 6.7 | 5.2 | 18.5 | 50 | 16.8 | 70.2 | 85.0 |
| MS5 | 12.5 | 64-22 | 6.3 | 4.7 | 21.9 | 30 | 16.0 | 68.8 | 87.9 |
| RR1 | | 64-22 | 5.8 | 4.6 | 21.1 | 30 | 15.7 | 68.2 | 89.5 |
| MS6 | | 76-22 | 6.5 | 5.0 | 22.7 | 50 | 16.8 | 70.2 | 85.7 |
| MS2 | 19 | 64-22 | 5.1 | 4.0 | 23.8 | 50 | 14.7 | 66.0 | 98.6 |
| MS3 | | 70-22 | 5.1 | 4.0 | 23.8 | 50 | 14.7 | 66.0 | 98.6 |
| EB2 | 25 | 64-22 | 4.5 | 3.9 | 22.0 | 50 | 14.0 | 64.3 | 85.0 |
| EB3 | | 70-22 | 4.7 | 4.1 | 20.9 | 30 | 14.4 | 65.3 | 83.1 |

TABLE 3.2
**Mix design information of collected SP 4 mixtures**

| Mix ID | NMAS (mm) | PG | $P_b$ | $P_{be}$ | % RAP (ABR) | $N_{des}$ | VMA | VFA | TSR |
|--------|-----------|-------|-------|----------|-------------|-----------|------|------|------|
| SP 4-9.5 | 9.5 | 64-22 | 6.1 | 4.9 | 22.5 | 75 | 15.6 | 74.4 | 92.7 |
| SP 4-12.5 | 12.5 | 64-22 | 6.0 | 4.6 | 20.7 | 100 | 14.7 | 72.8 | 96.0 |

**TABLE 3.3**
**Information on selected projects for field cores**

| Road | PG | Construction |
|------|-----|--------------|
| US 231 | 70-22 | June 27 to September 17, 2018 |
| US 30 | 76-22 | September 4 to December 2, 2018 |
| US 31 | 76-22 | June 6 to July 19, 2018 |



**Figure 3.1** Wire mesh holder preventing the collapse of the samples during aging.

aging, and 12 days of aging were established to assess the aging effect of SP 5 and SP 4 in this study. Samples selected for testing were fabricated and subsequently subjected to aging at 85°C for 5 days and 12 days, respectively, following AASHTO R 30 guidelines. To prevent the collapse of the sample due to heating, a wire mesh holder was used (Valentová et al., 2016). Figure 3.1 shows the wire mesh holder that was used in this study.

## 3.3 Sample Preparation of Mixture Testing

Specimens for all mixture tests were produced to achieve 7% air voids for SP 4 mixtures and 5% air voids for SP 5 mixtures, determined through an air void study for each mixture. The determination of air voids took into account the in-place density specifications of each mixture.

### 3.3.1 Sample Preparation for Dynamic Modulus Test and Fatigue Test

To conduct dynamic modulus and fatigue tests for assessing the aging effect of SP 5 and SP 4 mixtures and to generate material input for Pavement-ME, specimens were fabricated. Cylindrical specimens with dimensions of 38 mm in diameter and 110 mm in height were produced following AASHTO PP 99 guidelines. As depicted in Figure 3.2, four uncut samples, each with a diameter of 38 mm, were extracted from a gyratory pill measuring 150 mm in diameter and 180 mm in height, using a core machine. Subsequently, these samples were sawed to a height of 110 mm.

### 3.3.2 Sample Preparation for HWTT

Hamburg Wheel Track Testing (HWTT) specimens were prepared to evaluate the rutting performance difference between SP 5 and SP 4 based on aging effects. Two specimens were extracted from a gyratory pill. The top and bottom sides of a pill with a height of 180 mm were removed, and two test specimens with a height of 50 mm were taken from the middle to obtain samples with evenly distributed air voids. As illustrated in Figure 3.3, one end was cut to ensure that the two specimens fit together.

## 3.4 Sample Preparation for Binder Testing

### 3.4.1 Binder Extraction and Recovery

The extraction procedure was done per the ASTM D2172 specification (ASTM, 2011). In this method, the sample was loosened by using an oven at 110°C ± 5°C. Then 2,000 grams of loose asphalt mix was placed in the extraction bowl (see Figure 3.4). A sufficient amount of N-propyl bromide (nPB) was poured into the bowl to fill it up and then allowed for sufficient time (around 1 hour) to dissolve the asphalt binder into the nPB solution. Afterward, the bowl was placed into the extractor. A glass beaker was placed to receive the extracted binder solution. After securing the chamber cover, the extractor started to rotate. The rotation speed was increased slowly up to 3,000 rpm. The device was kept running until the extract ceased its flow from the ejection pipe. Around 2–3 washes were conducted using nPB to collect all the binders. Then the extracted sample was allowed to rest for about 15 minutes to settle the fine particles, and then carefully transferred to a flask for recovery.

A rotavapor was used to recover the asphalt binder from the previously extracted nPB solution (Figure 3.5). The recovery procedure was performed per the ASTM D5404 specification (2012). In this method, the rotavapor was used to evaporate nPB from the solution and subsequently cooled it down to liquid form using a condenser, leaving the asphalt binder in the original flask. At first, the flask was fitted appropriately, and the oil bath was heated at a temperature of 140 ± 3°C. The coolant was then run through the condenser while the flask was set to rotate at approximately 40 rpm. A vacuum pressure of 5.3 ± 0.7 kPa below the atmospheric pressure was applied to the flask, and nitrogen gas was supplied to the flask at a rate of approximately 500 mL/min. At these conditions, controlled evaporation of about 100 mL/min was maintained. Once the bulk amount of nPB is removed, the high-speed centrifuge is used to remove the fine particles. Then, the vacuum pressure slowly increased up to 80.0 ± 0.7 kPa below the atmospheric pressure, and the nitrogen supply was adjusted to approximately 600 mL/min with a rotation speed of 45 rpm. The vacuum pressure was adjusted if any foaming or bubble formation was noticed in the flask. After the formation of the last

**Figure 3.2** Testing specimen fabrication process.
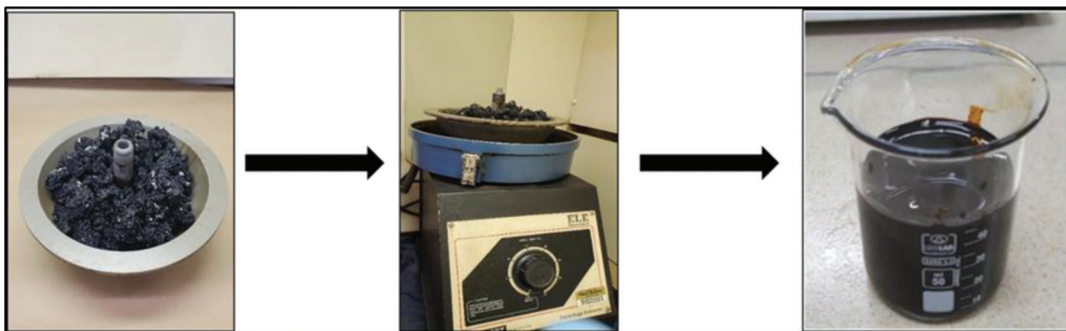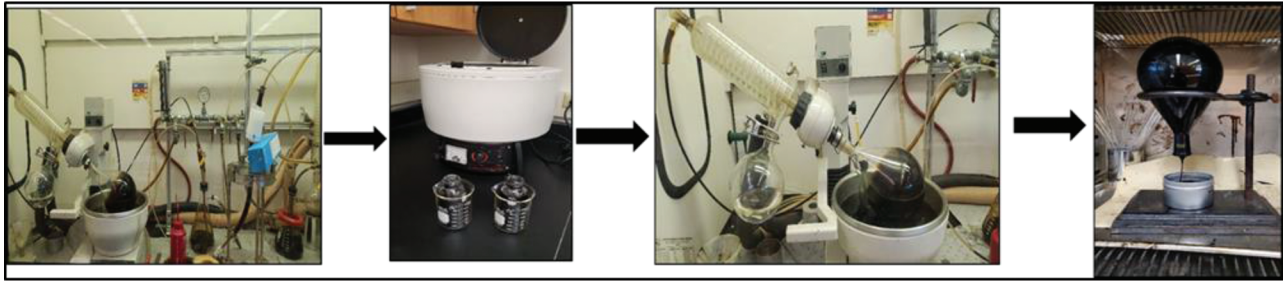


**Figure 3.3** HWTT specimen fabrication.



**Figure 3.4** Extraction of asphalt binders using a centrifuge extractor.

**Figure 3.5** Asphalt binder recovery using rotavapor.

bubble, the setup was run for 10 minutes. After 10 minutes, the rotation of the flask was stopped slowly; the flask was removed and placed upside down in an appropriate-sized container to transfer the binder to the container. The flask-container setup was kept in an oven at a temperature of 130°C for a quick transfer of asphalt binder to the container.

## 4. LABORATORY TESTING

### 4.1 Asphalt Mixture Testing

#### 4.1.1 Dynamic Modulus Test

Dynamic modulus is a crucial parameter for evaluating the performance of asphalt mixtures and is integral to flexible pavement design using the *Mechanistic-Empirical Pavement Design Guide* (MEPDG). In this study, the dynamic modulus test was chosen to assess the performance difference between SP 5 and SP 4 due to aging effects, as part of the mixture performance test. The results of the dynamic modulus test will also be employed to adjust the input parameters for the SP 5 mix in MEPDG pavement design.

For each mixture and aging level, four replicates were prepared for dynamic modulus and cyclic fatigue tests. SP 5 specimens were crafted with $5 \pm 0.5\%$ air voids, while SP 4 specimens were made with $7 \pm 0.5\%$ air voids. The air voids of each specimen for dynamic modulus and fatigue tests are detailed in Table 4.1.

Tests were conducted at three different temperatures (4°C, 20°C, and 40°C) and three distinct frequencies (0.1 Hz, 1.0 Hz, and 10 Hz) using the Asphalt Mixture Performance Tester (AMPT) in accordance with AASHTO TP 132. The test results are presented in Table 4.2.

The dynamic moduli at various temperatures obtained from the Asphalt Mixture Performance Tester (AMPT) test results were fitted to a master curve using FlexMAT for cracking, an Excel-based analysis tool for characterizing dynamic modulus and cracking of asphalt mixtures. Figure 4.1 displays the master curves for SP 4-9.5 and MS1 with the NMAS of 9.5 mm at different aging levels. As anticipated, the dynamic moduli of both mixtures increased with aging, confirming that the stiffness of the asphalt binder heightened as oxidation progressed. However, as depicted in Figure 4.1, a distinct difference in the modulus increment with aging between the two mixtures was

TABLE 4.1
**Dynamic modulus and fatigue test specimen air void contents**

| Mix | Aging | Air Voids (%) | | | | Average |
|-----|-------|---|---|---|---|---------|
| | | 1 | 2 | 3 | 4 | |
| SP 4-9.5 | Unaged | 6.91 | 7.03 | 6.92 | 7.19 | 7.01 |
| | 5 days | 6.99 | 6.92 | 7.16 | 6.83 | 6.98 |
| | 12 days | 6.90 | 7.13 | 6.91 | 6.95 | 6.97 |
| SP 4-12.5 | Unaged | 7.41 | 7.01 | 6.95 | 6.98 | 7.09 |
| | 5 days | 6.79 | 7.20 | 6.65 | 7.00 | 6.91 |
| | 12 days | 7.17 | 7.28 | 6.66 | 6.92 | 7.01 |
| MS1 | Unaged | 5.29 | 5.26 | 4.73 | 4.61 | 4.97 |
| | 5 days | 5.03 | 4.77 | 5.07 | 4.76 | 4.91 |
| | 12 days | 4.75 | 4.81 | 5.02 | 5.05 | 4.91 |
| RR1 | Unaged | 5.26 | 4.74 | 4.84 | – | 4.95 |
| | 5 days | 5.24 | 4.70 | 5.01 | – | 4.98 |
| | 12 days | 4.94 | 5.29 | 4.80 | – | 5.01 |
| EB4 | Unaged | 4.90 | 4.90 | 4.79 | 5.07 | 4.92 |
| | 5 days | 5.11 | 5.04 | 5.25 | 4.71 | 5.03 |
| | 12 days | 5.10 | 5.26 | 4.94 | 5.28 | 5.15 |

evident. This discrepancy can be attributed to differences in the degree of aging resulting from differences in air voids between the two mixtures.

To examine more quantitative differences, as depicted in Figure 4.2, the dynamic modulus of SP 4-9.5 and MS1 at a temperature of 40°C and a frequency of 0.1 Hz was compared. This specific temperature and frequency were chosen as the effects of aging are most pronounced under high temperatures and low frequencies. The modulus of SP 4-9.5 after 5 days of aging was 591.4 kPa, reflecting an increase of approximately 183.0% compared to 323.2 kPa in the unaged condition. Following 12 days of aging, the modulus further increased to 788.9 kPa, marking a final increment of about 244.1% compared to the unaged modulus.

Conversely, MS1 exhibited a modulus increase of about 141.4% from 349.7 kPa to 491.8 kPa after 5 days of aging. After 12 days of aging, the modulus experienced a further rise of 204.8%, reaching 712.3 kPa compared to the unaged modulus. The dynamic modulus test results indicate that SP 5, due to smaller air voids exhibits a slower increase in stiffness due to aging compared to SP 4, thereby providing the advantage of enhanced cracking resistance.

TABLE 4.2
**Dynamic modulus test results**

| Mix | Aging Level | Temperature (°C) | Frequency | | |
|---|---|---|---|---|---|
| | | | 0.1 Hz | 1 Hz | 10 Hz |
| SP 4-9.5 | UA | 4 | 8,735.6 | 11,899.1 | 1,5142.1 |
| | | 20 | 2,444.0 | 4,587.6 | 7,368.7 |
| | | 40 | 323.2 | 806.9 | 1,844.2 |
| | 5D | 4 | 10,870.5 | 13,968.0 | 16,974.1 |
| | | 20 | 3,514.4 | 5,957.9 | 8,905.6 |
| | | 40 | 5,91.4 | 1,290.3 | 2,603.8 |
| | 12D | 4 | 11,710.8 | 14,580.0 | 17,331.4 |
| | | 20 | 4,351.0 | 6,873.5 | 9,737.7 |
| | | 40 | 788.9 | 1,609.3 | 3,041.6 |
| SP 4-12.5 | UA | 4 | 8,587.1 | 11,613.0 | 14,556.2 |
| | | 20 | 2,578.1 | 4,619.9 | 7,316.9 |
| | | 40 | 450.4 | 972.0 | 1,991.1 |
| | 5D | 4 | 9,701.3 | 12,719.9 | 15,661.8 |
| | | 20 | 3,147.1 | 5,368.5 | 8,144.3 |
| | | 40 | 565.5 | 1,192.7 | 2,361.2 |
| | 12D | 4 | 10,787.0 | 13,640.5 | 16,408.4 |
| | | 20 | 3,895.8 | 6,217.7 | 8,947.0 |
| | | 40 | 756.6 | 1,513.4 | 2,824.4 |
| MS1 | UA | 4 | 10,169.6 | 13,650.9 | 17,099.9 |
| | | 20 | 2,946.0 | 5,569.5 | 8,839.5 |
| | | 40 | 347.9 | 911.4 | 2,166.4 |
| | 5D | 4 | 11,452.9 | 14,784.3 | 17,982.9 |
| | | 20 | 3,725.0 | 6,596.8 | 9,940.7 |
| | | 40 | 491.8 | 1,212.8 | 2,707.2 |
| | 12D | 4 | 12,708.9 | 15,899.0 | 19,000.0 |
| | | 20 | 4,729.0 | 7,653.4 | 10,866.2 |
| | | 40 | 712.3 | 1,638.5 | 3,361.5 |
| RR1 | UA | 4 | 8,184.6 | 11,877.5 | 15,659.4 |
| | | 20 | 1,917.7 | 4,023.3 | 7,092.3 |
| | | 40 | 222.0 | 594.9 | 1,486.1 |
| | 5D | 4 | 9,655.3 | 13,173.4 | 16,649.2 |
| | | 20 | 2,580.6 | 4,980.1 | 8,152.2 |
| | | 40 | 334.2 | 842.7 | 1,963.6 |
| | 12D | 4 | 10,670.2 | 14,008.7 | 17,297.1 |
| | | 20 | 3,290.4 | 5,829.7 | 8,947.7 |
| | | 40 | 482.6 | 1,137.3 | 2,450.9 |
| EB4 | UA | 4 | 10,509.5 | 13,895.5 | 17,057.3 |
| | | 20 | 3,263.8 | 5,858.0 | 9,126.0 |
| | | 40 | 509.3 | 1,141.7 | 2,413.7 |
| | 5D | 4 | 11,327.6 | 14,542.4 | 17,539.1 |
| | | 20 | 3,987.8 | 6,729.6 | 9,961.0 |
| | | 40 | 678.4 | 1,463.2 | 2,940.9 |
| | 12D | 4 | 11,918.6 | 15,055.6 | 17,976.1 |
| | | 20 | 4,661.6 | 7,481.7 | 10,682.7 |
| | | 40 | 861.8 | 1,768.3 | 3,376.7 |

The master curves of two mixtures, SP 4-12.5 and RR1 with a Nominal Maximum Aggregate Size (NMAS) of 12.5 mm, were also compared, as illustrated in Figure 4.3. The dynamic moduli of both mixtures increased with aging. However, unlike the cases of SP 4-9.5 and MS1, RR1 exhibited a slightly larger increase in modulus than SP 4-12.5 due to aging, despite having smaller air voids. Moreover, even though the two mixtures shared the same NMAS of 12.5 mm and the same Performance Grade (PG) of 64-22, the overall modulus of SP 4-12.5 was significantly higher than that of RR1. This result differed from expectations, as the benefits of SP 5 were not evident at all.

To investigate the cause of this discrepancy, the research team compared the moduli of unaged specimens for all mixtures. EB4 is a mixture using PG 76-22 which is a modified asphalt binder, while all other mixtures use PG 64-22 binder. However, Figure 4.4 reveals an unexpected trend. The results presented in Figure 4.4 represent the modulus master curves of unaged specimens, excluding the effects of aging. The curves of SP 4-9.5, MS1, and RR1 are closely aligned. However, the curve of SP 4-12.5 deviated significantly from the same PG 64-22 group and closely resembled the curve of PG 76-22. This suggests that the binder of SP 4-12.5 had a higher viscosity than PG 64-22. This trend is also evident in the binder test results discussed in Section 4.2. Therefore, the test results of SP 4-12.5 were excluded from this study since it is not comparable with RR1 due to different PGs.

As depicted in Figure 4.5, the modulus master curves of two SP 5 mixtures, MS1 with PG 64-22 and EB4 with PG 76-22, were compared to observe the effect of aging based on the binder type. As anticipated, EB4 with PG 76-22, a modified asphalt binder, exhibited a higher modulus than MS1 with PG 64-22. The distinction in aging effect between the two mixes, attributable to the difference in the Performance Grade (PG) of the binder, is evident in Figure 4.6.

Figure 4.6 illustrates the increase in modulus for MS1 and EB4 due to aging at a temperature of 40°C and a frequency of 0.1 Hz. In the case of MS1, the modulus increased to 491.8 kPa and 712.3 kPa after 5 days and 12 days of aging, respectively. Relative to the unaged modulus, the increase rates were 141.4% and 204.8%, respectively. Conversely, the 5-day aging modulus of EB4 was 678.4 kPa, marking an increase of 133.2% compared to the unaged modulus of 509.3 kPa. The modulus after 12 days of aging was 861.8 kPa, reflecting an increase of 169.2%. This represents a significantly lower rate of increase than that observed in MS1 due to aging, highlighting that the mixture with a high-viscosity modified asphalt is less sensitive to aging than the mixture with a general asphalt binder.
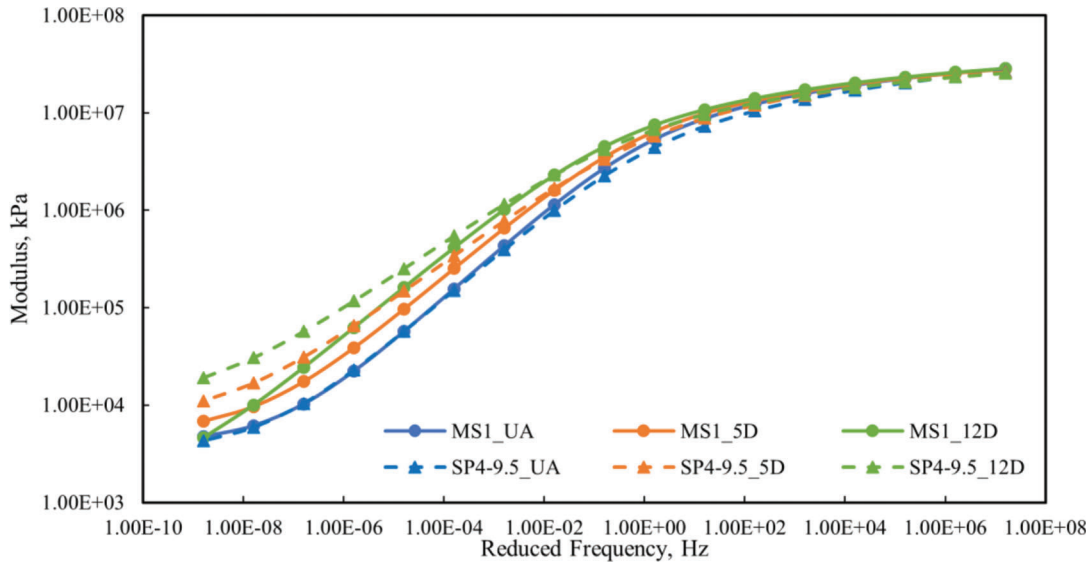
**Figure 4.1** Dynamic modulus master curves of SP 4-9.5 and MS1 at different aging levels.
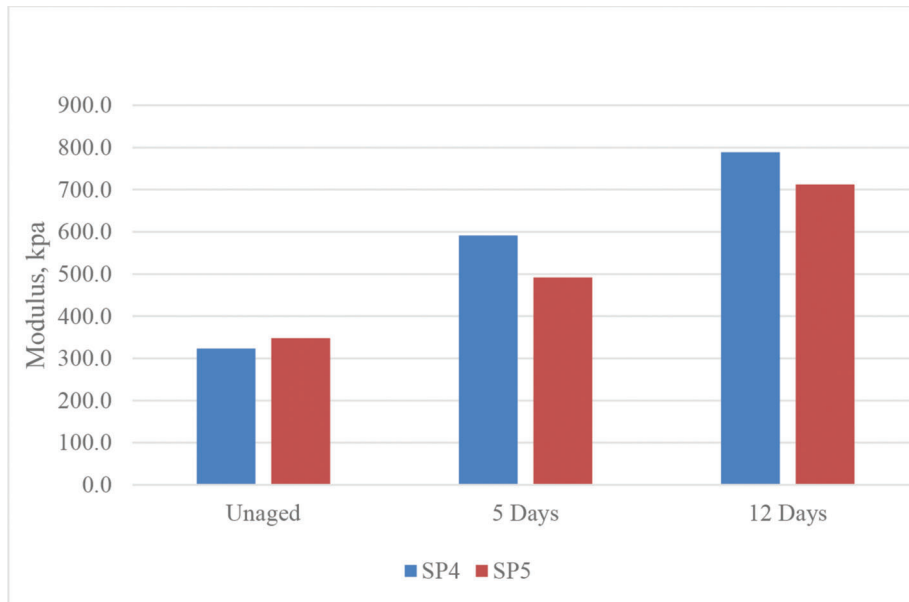


**Figure 4.2** Dynamic modulus of SP 4-9.5 and MS1 at a temperature of 40°C and a frequency of 0.1 Hz.

### 4.1.2 HWTT

The HWTT is perhaps the most widely used laboratory test method for evaluating asphalt mixture rut resistance. The standard test procedure is *AASHTO T324-19, Hamburg Wheel-Track Testing of Compacted Asphalt Mixtures*. Compacted slab specimens or two cylindrical specimens are placed in the machine, submerged in a heated water bath, and tested in accordance with the method as shown in Figure 4.7. The HWTT is a destructive test method that measures the rut depths of compacted asphalt specimens that are subjected to continuous loading imposed by a 47 mm wide, 705 N steel wheel for 20,000 passes. The recorded rut depth provides a direct indication of a mixture's rutting resistance and the stripping inflection point.

HWTT was performed on only one mixture each for SP 5 (MS1) and SP 4 (SP 4-9.5) to evaluate differences in rutting performance due to aging effects. For HWTT, two replicates were prepared for each mixture and aging level. Table 4.3 shows the air voids of each specimen for HWTT. SP 4 specimens were prepared with $7 \pm 0.5\%$ air voids, and SP 5 specimens were prepared with $5 \pm 0.5\%$ air voids.

Figure 4.8 illustrates the progression of rut depth for the two mixtures at different aging levels as the number of wheel passes progresses. At all aging levels, the rut depth of SP 4 was greater than that of SP 5. This is
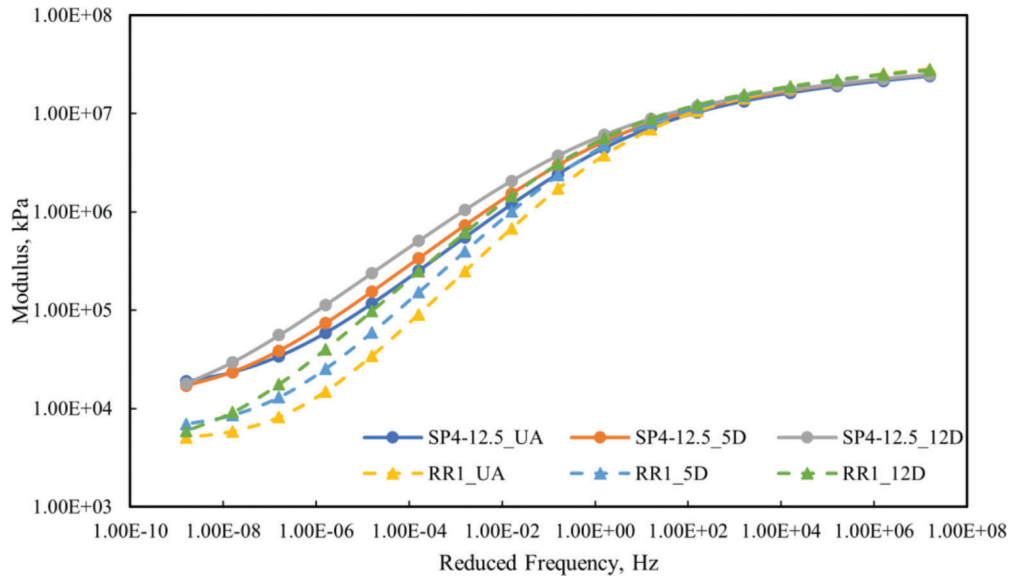
**Figure 4.3** Dynamic modulus master curves of SP 4-12.5 and RR1 at different aging levels.
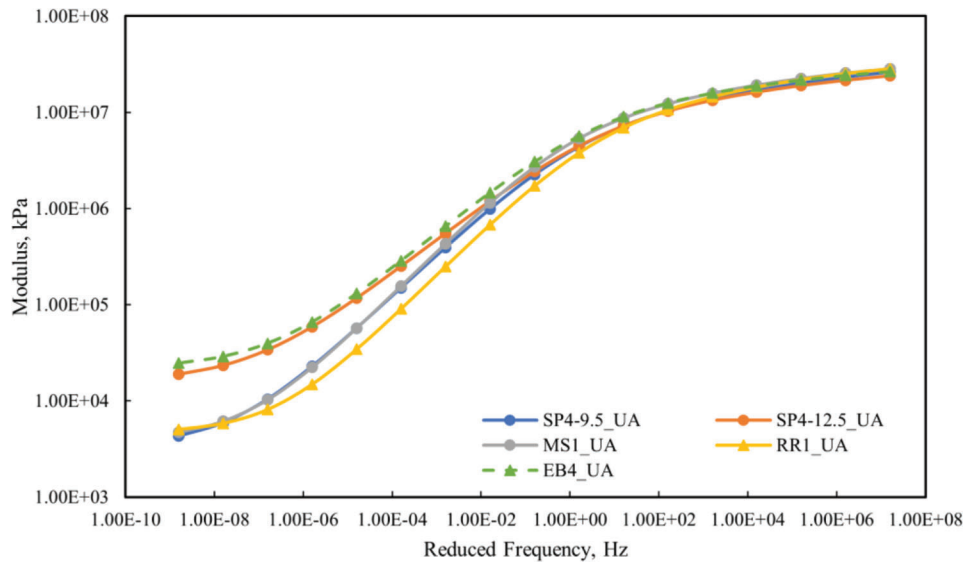


**Figure 4.4** Dynamic modulus master curves of unaged specimens for all mixtures.

attributed to the higher air voids of SP 4, indicating lower rutting resistance. Additionally, both mixtures exhibited a tendency for decreasing rut depth as stiffness increased with aging progression.

Figure 4.9 presents the rut depths of SP 4 and SP 5, along with the rut depth difference between the two mixtures after 20,000 passes. In the unaged condition after 2,000 passes, the rut depths were 3.96 mm and 2.89 mm for SP 4 and SP 5, respectively, with a difference of 1.07 mm. After 5 days of aging, the rut depths were 3.38 mm and 2.58 mm, respectively, and the difference decreased to 0.8 mm. After 12 days of aging, the difference in rut depth between the two mixtures further decreased to 0.13 mm, indicating almost similar rut depths. This result highlights increased resistance to rutting in SP 4 compared to SP 5 as SP 4

undergoes more aging due to its higher air voids, leading to a significant increase in stiffness compared to SP 5.

### 4.1.3 Cyclic Fatigue Test

Fatigue cracking is one of the main distress types of asphalt pavement, and as the asphalt mix ages, the binder becomes stiffer, significantly affecting the cracking of asphalt mixtures by reducing the relaxation capability (Zhang et al., 2020). Therefore, the degree of aging can be determined through a cracking test. Thus, a cyclic fatigue test was performed to evaluate the difference in aging between SP 4 and SP 5. In this study, the specimens used in the dynamic modulus test were reused in the fatigue test. Fatigue testing was performed at a
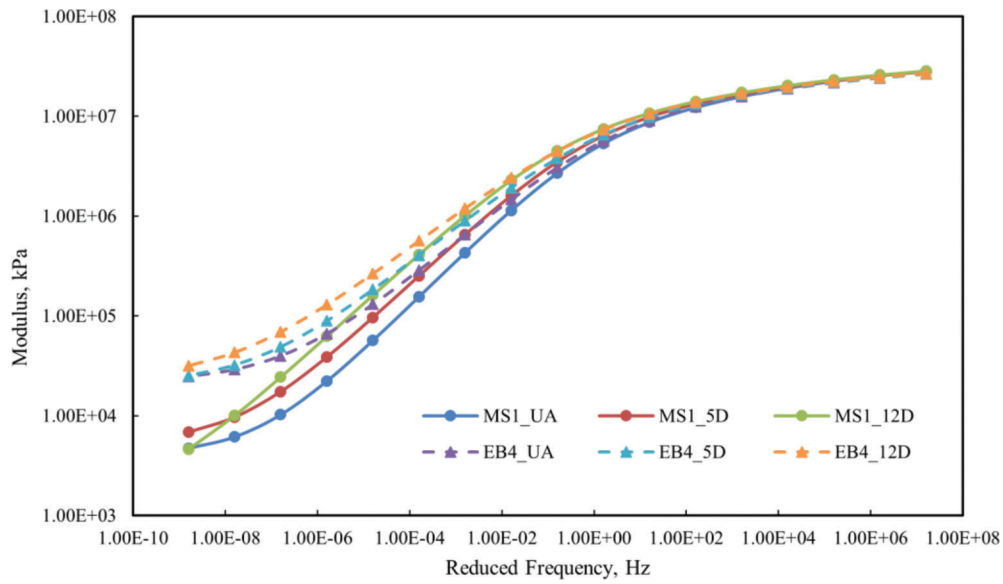
**Figure 4.5** Dynamic modulus master curves of MS1 and EB4.
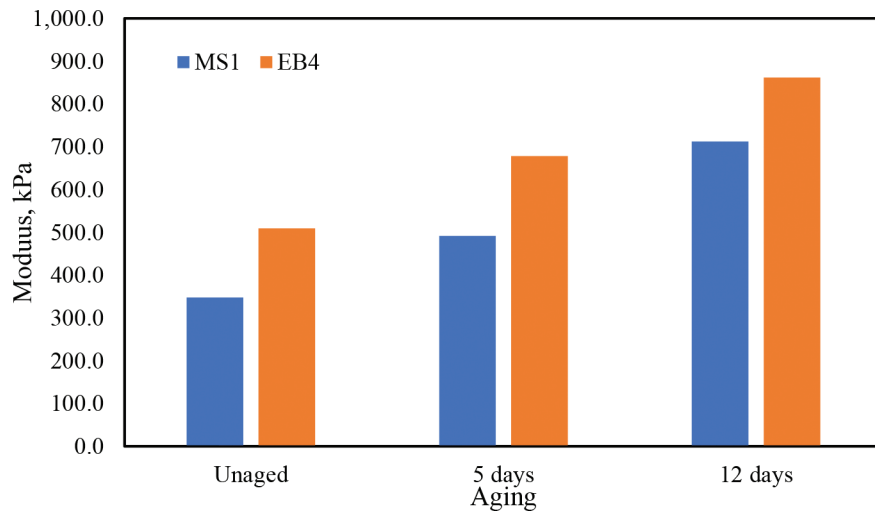


**Figure 4.6** Dynamic modulus of MS1 and EB4 at a temperature of 40°C and at a frequency of 0.1 Hz.



**Figure 4.7** INDOT HWTT set up.

TABLE 4.3
**Air voids of each specimen for HWTT**

| Mix | Aging | Replicate | AV | Mix | Aging | Replicate | AV |
|---|---|---|---|---|---|---|---|
| SP 4-9.5 | Unaged | 1 | 7.07 | MS1 | Unaged | 1 | 5.09 |
| | | 2 | 7.04 | | | 2 | 5.10 |
| | 5 days | 1 | 6.87 | | 5 days | 1 | 5.05 |
| | | 2 | 7.16 | | | 2 | 4.97 |
| | 12 days | 1 | 7.07 | | 12 days | 1 | 5.09 |
| | | 2 | 6.82 | | | 2 | 4.96 |
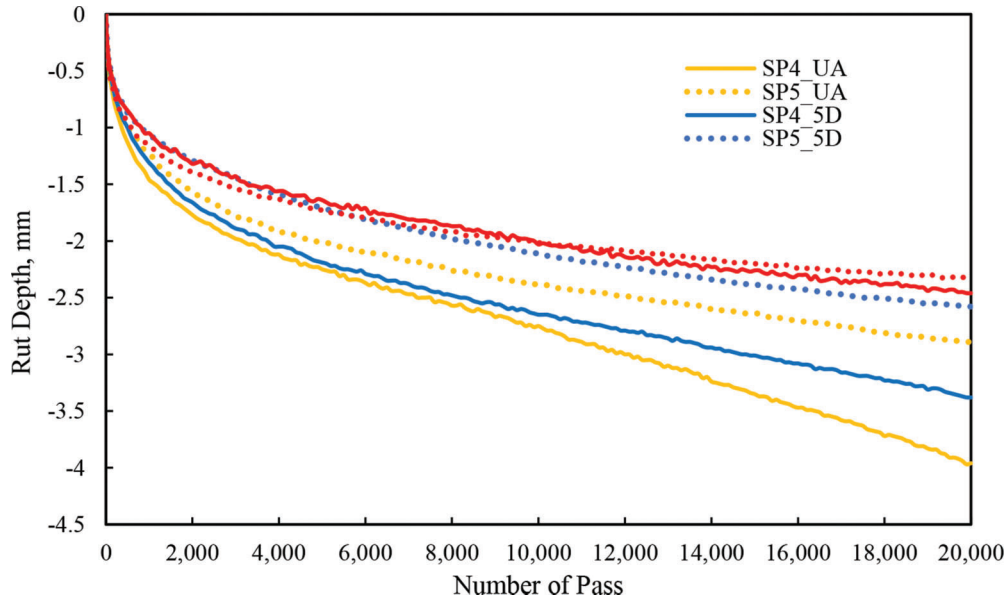


**Figure 4.8** Rut depth progression of SP 5 and SP 4 at different aging levels.
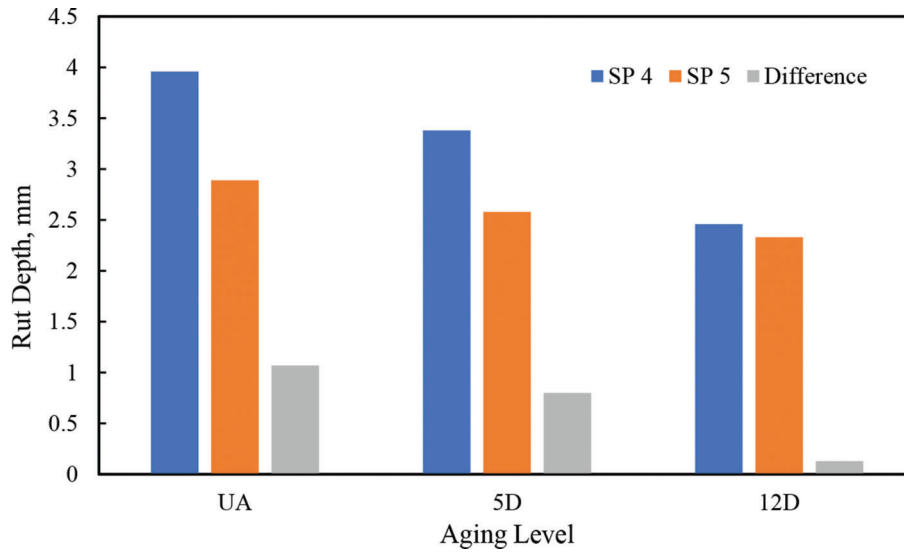


**Figure 4.9** Rut depth after 20,000 passes.

temperature of 18°C for PG 64-22 and 21°C for PG 76-22, and a frequency of 10 Hz using AMPT in accordance with AASHTO TP 133. Table 4.4 shows the summary of fatigue test results.

The $D^R$ is the fatigue failure criterion developed by North Carolina State University (NCSU). It is used to predict material failure in the simplified viscoelastic continuum damage (S-VECD) model and is based on the observation that the average reduction in pseudo stiffness up to failure is independent of the mode of loading, temperature, and load amplitude (Wang & Kim, 2017). Criterion $D^R$ is defined by the slope of the linear relationship between the sum of $(1-C)$ to failure and the number of cycles to failure ($N_f$). Good trends were observed for $D^R$ according to aging. The $D^R$ value of both SP 4-9.5 and MS1 decreased as they aged. After 12 days of aging, the $D^R$ of SP 4-9.5 decreased by about 11.7%, the $D^R$ of MS1 decreased by about 12.0%, and the two mixtures showed similar reduction rates. The $D^R$ value alone cannot be used to compare the fatigue resistance of different asphalt mixtures because it measures toughness without consideration of the modulus (Etheridge et al., 2019).

The cyclic fatigue index parameter, $S_{app}$, was developed by NCSU to represent fatigue cracking resistance in a single parameter. It is based on concepts of the S-VECD model. $S_{app}$ accounts for the effects of a material's modulus and toughness on its fatigue resistance and is a measure of the amount of fatigue damage the material can tolerate under loading. Higher $S_{app}$ values indicate better fatigue resistance of the mixture. Test results showed good trends for $S_{app}$. In both mixtures, $S_{app}$ values tended to decrease with aging indicating a decrease in cracking resistance due to aging. In the case of the rate of decrease in $S_{app}$ value due to aging, SP 4-9.5 decreased by about 30.6% compared to unaged after 12 days of aging, while MS1 showed a decrease rate of only about 15.8%, which is approximately half of the decrease rate of SP 4-9.5. Therefore, it can be seen that SP 4-9.5, which has higher air voids, has a greater decrease in cracking resistance compared to MS1 due to a greater aging effect.

TABLE 4.4
Summary of fatigue test results

| Specimen ID | | Fingerprint \|E*\| (MPa) | DMR | $N_f$ | log ($N_f$) | Cum. (1-C) | $D^R$ | Input Strain (μ) | $S_{app}$ |
|---|---|---|---|---|---|---|---|---|---|
| SP 4-9.5 | UA-1 | 8,656 | 1.06 | 11,750 | 4.07 | 6,680 | 0.569 | 350 | 26.37 |
| | UA-2 | 8,477 | 1.04 | 13,700 | 4.14 | 8,365 | 0.611 | 350 | 29.98 |
| | UA-3 | 8,624 | 1.06 | 23,090 | 4.36 | 13,626 | 0.590 | 350 | 30.30 |
| | UA$_{ave}$ | N/A | N/A | N/A | N/A | N/A | 0.590 | N/A | 28.88 |
| | 5D-1 | 9,271 | 0.96 | 6,470 | 3.81 | 3,506 | 0.542 | 320 | 21.52 |
| | 5D-2 | 8,948 | 0.92 | 20,320 | 4.31 | 10,925 | 0.538 | 300 | 21.12 |
| | 5D-3 | 9,796 | 1.01 | 6,840 | 3.84 | 3,725 | 0.545 | 300 | 21.00 |
| | 5D$_{ave}$ | N/A | N/A | N/A | N/A | N/A | 0.541 | N/A | 21.21 |
| | 12D-1 | 10,192 | 0.97 | 22,330 | 4.35 | 11,631 | 0.521 | 260 | 20.12 |
| | 12D-2 | 10,399 | 0.99 | 17,030 | 4.23 | 9,156 | 0.538 | 280 | 21.96 |
| | 12D-3 | 9,669 | 0.92 | 10,660 | 4.03 | 5,371 | 0.504 | 280 | 18.08 |
| | 12D$_{ave}$ | N/A | N/A | N/A | N/A | N/A | 0.521 | N/A | 20.05 |
| MS1 | UA-1 | 10,818 | 1.12 | 2,780 | 3.44 | 1,430 | 0.515 | 400 | 27.92 |
| | UA-2 | 9,814 | 1.02 | 53,570 | 4.73 | 23,823 | 0.445 | 270 | 21.60 |
| | UA$_{ave}$ | N/A | N/A | N/A | N/A | N/A | 0.480 | N/A | 24.76 |
| | 5D-1 | 11,085 | 1.03 | 12,000 | 4.08 | 5,692 | 0.474 | 300 | 23.62 |
| | 5D-2 | 11,605 | 1.08 | 35,580 | 4.55 | 15,136 | 0.425 | 250 | 19.29 |
| | 5D-3 | 11,002 | 1.02 | 27,970 | 4.45 | 12,271 | 0.439 | 270 | 20.50 |
| | 5D$_{ave}$ | N/A | N/A | N/A | N/A | N/A | 0.446 | N/A | 21.14 |
| | 12D-1 | 11,509 | 1.04 | 7,110 | 3.85 | 3,208 | 0.451 | 280 | 22.95 |
| | 12D-2 | 11,527 | 1.04 | 14,990 | 4.18 | 6,502 | 0.434 | 250 | 21.36 |
| | 12D-3 | 12,072 | 1.09 | 93,090 | 4.97 | 33,244 | 0.357 | 220 | 17.91 |
| | 12D$_{ave}$ | N/A | N/A | N/A | N/A | N/A | 0.422 | N/A | 20.84 |
| EB4 | UA-1 | 8,163 | 0.94 | 53,300 | 4.73 | 32,033 | 0.601 | 350 | 32.81 |
| | UA-2 | 8,561 | 0.98 | 17,920 | 4.25 | 11,525 | 0.643 | 400 | 37.80 |
| | UA-3 | 8,595 | 0.99 | 15,490 | 4.19 | 10,162 | 0.656 | 450 | 45.35 |
| | UA$_{ave}$ | N/A | N/A | N/A | N/A | N/A | 0.633 | N/A | 38.65 |
| | 5D-1 | 9,584 | 1.01 | 88,000 | 4.94 | 55,207 | 0.627 | 320 | 40.52 |
| | 5D-2 | 8,894 | 0.93 | 21,990 | 4.34 | 12,739 | 0.579 | 360 | 30.29 |
| | 5D-3 | 8,868 | 0.94 | 6,710 | 3.83 | 3,829 | 0.571 | 420 | 30.71 |
| | 5D$_{ave}$ | N/A | N/A | N/A | N/A | N/A | 0.592 | N/A | 33.84 |
| | 12D-1 | 10,507 | 1.03 | 4,510 | 3.65 | 2,583 | 0.573 | 400 | 33.90 |
| | 12D-2 | 9,382 | 0.92 | 21,490 | 4.33 | 11,986 | 0.558 | 360 | 28.12 |
| | 12D$_{ave}$ | N/A | N/A | N/A | N/A | N/A | 0.565 | N/A | 31.01 |

When comparing MS1 and EB4, which are the same SP 5 mixtures with different binders, the rate of decrease in Sapp value due to aging was 15.8% and 19.8%, respectively, showing no significant difference. However, the numerical value of Sapp between the two mixtures is significantly different. This confirmed that the PG 76-22 binder showed significantly better cracking performance than the PG 64-22 binder.

## 4.2 Asphalt Binder Testing

### 4.2.1 Dynamic Shear Modulus Test

The DSR test is performed to measure the complex shear modulus (G*) and phase angle (δ) at different temperatures to characterize the viscous and elastic behavior of the asphalt binder. The G* is the measure of the total resistance of the binder to deformation and the δ is the measure of the elasticity of the binder (Hossain et al., 2020). The lower values of δ indicate that the binder is more elastic, whereas a higher value indicates a viscous binder. In this research, an Anton Paar MCR 302 DSR machine was used. For the DSR test, a thin binder sample with a diameter of 25 mm is sandwiched between two circular plates. The lower plate is fixed, and the upper plate oscillates back and forth and creates a shearing action. The test frequency is 10 radians per second (1.59 Hz) as per AASHTO T 315 (2010). The test is performed according to AASHTO T 315 in different aging conditions of the binders.

In this study, DSR tests were conducted at several temperatures. Figures 4.10 and 4.11 showed the G* results at different temperatures at three aging levels. G* results showed an increasing trend due to aging. As the asphalt binders became stiffer because of long-term aging, the G* results showed higher values in 5-day and 12-day aging conditions (Bagchi et al., 2021; Zhang et al., 2018). The G* values at different temperatures and the phase angle are the inputs for the Pavement ME simulation. Figure 4.10 shows the G* values at different temperatures of MS1 (64-22-9.5) and RR1 (64-22-12.5). MS1 showed higher G* values than the RR1 though the PG grade is the same. The reason is the binder replacement percent is higher for MS1.
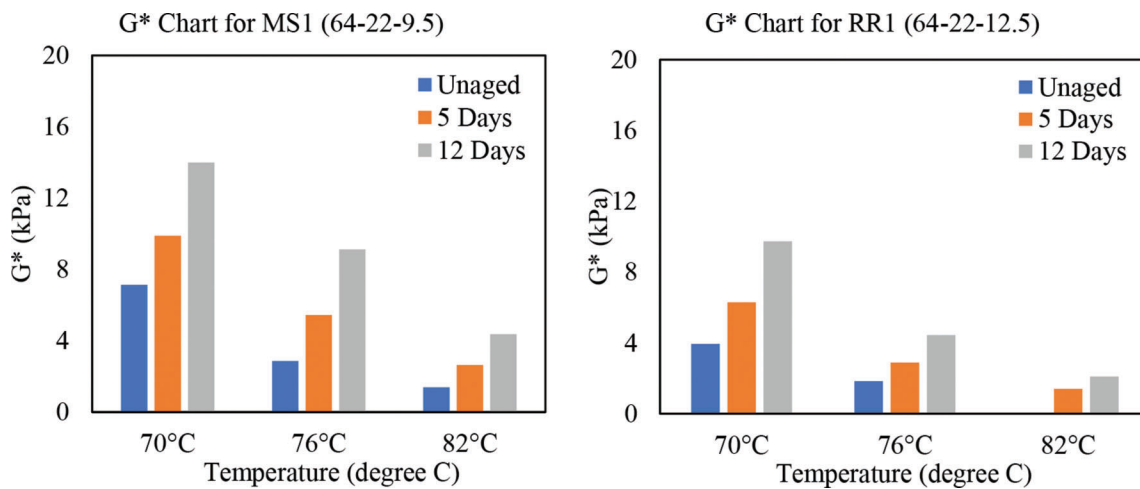


**Figure 4.10**   G* values of MS1 and RR1 at different aging levels.
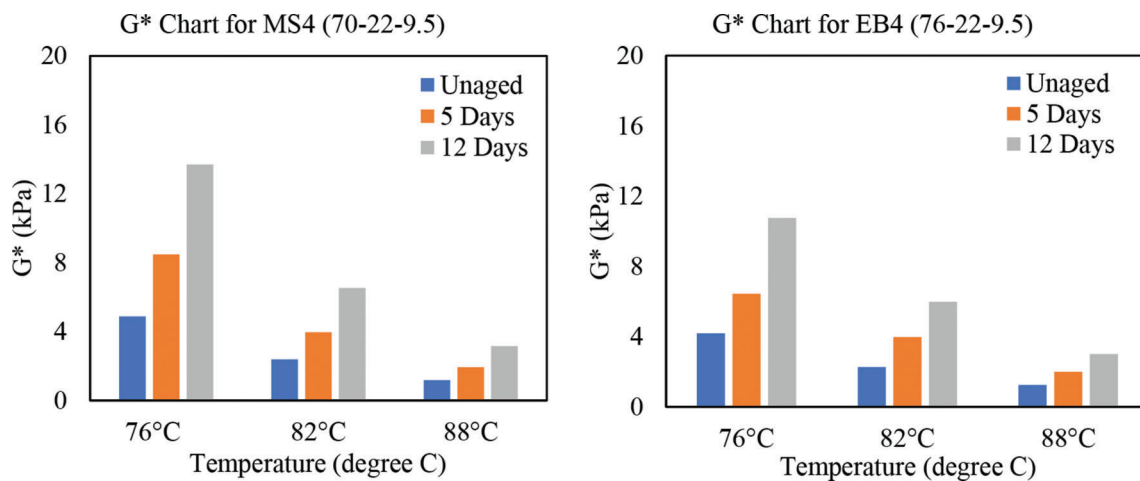


**Figure 4.11**   G* values of MS4 and EB4 at different aging levels.

Figure 4.11 shows the G* values at different temperatures of MS4 (70-22-9.5) and EB4 (76-22-9.5). MS4 showed higher G* values than the EB4 though EB4 has a higher PG grade. The reason is the binder replacement percent for EB4 is only 18.5% whereas the binder replacement of MS4 is 23.6%. In unaged conditions, MS4 shows a higher G* value than EB4, and after aging, the MS4 shows a higher trend as well.

In this study, two SP 4 samples were tested for DSR, and the G* values were compared with SP 5 samples. Both SP 4 and SP 5 have the same PG (i.e., PG 64-22) with a different NMASs of 9.5 mm and 12.5 mm, respectively. Figure 4.12 shows the G* comparison between SP 4 and SP 5 with NMAS 9.5. It is evident that the SP 4 shows higher G* due to aging than the SP 5 sample. For SP 5, the increment from unaged to

5 days is 38% whereas the increment for SP 4 is 40%. In addition, for SP 5, the increment from 5 days to 12 days is 42% whereas the increment for SP 4 is 65%. Figure 4.13 shows the G* comparison between SP 4 and SP 5 with NMAS 12.5. It is found that the SP 4 shows higher G* due to aging than the SP 5 sample. Figure 4.13 shows that for SP 5, the increment from unaged to 5 days is 57% whereas the increment for SP 4 is 60%. In addition, for SP 5, the increment from 5 days to 12 days is 53% whereas the increment for SP 4 is 65%. From this analysis, it is evident that the SP 4 sample has undergone more aging than the SP 5 sample in the same aging condition. The main reason is the higher air void percentage in SP 4 which leads to more oxidative aging.

Figure 4.14 shows the G* results of the collected three field core samples. All three routes were constructed
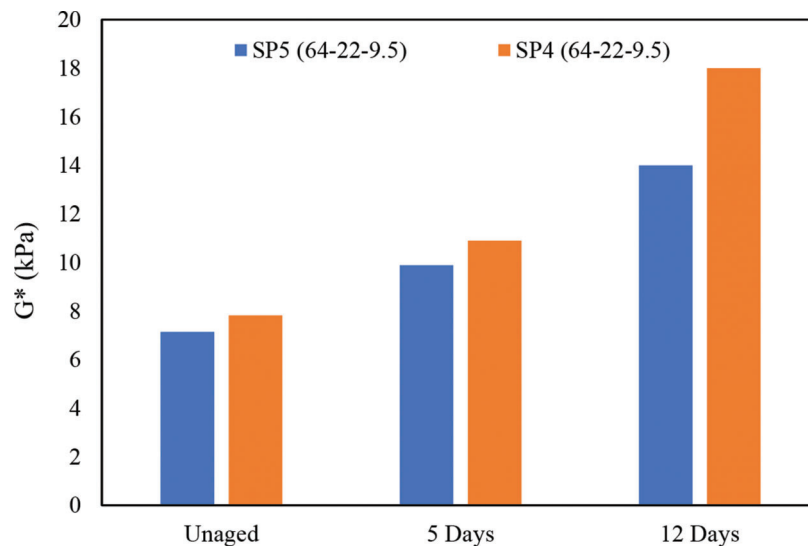


**Figure 4.12**   G* comparison between SP 5 (64-22-9.5) and SP 4 (64-22-9.5).
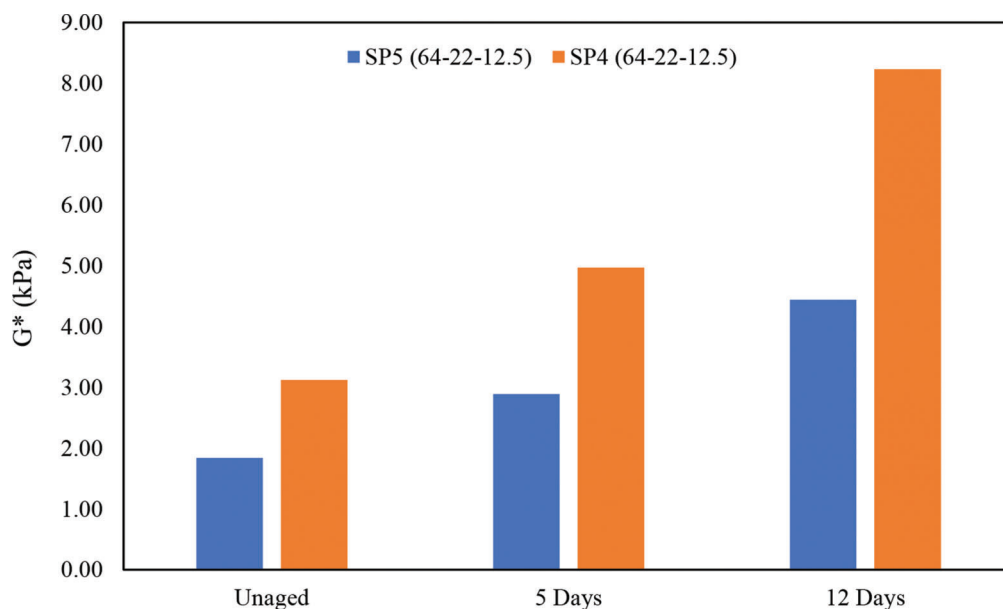


**Figure 4.13**   G* comparison between SP 5 (64-22-12.5) and SP 4 (64-22-12.5).
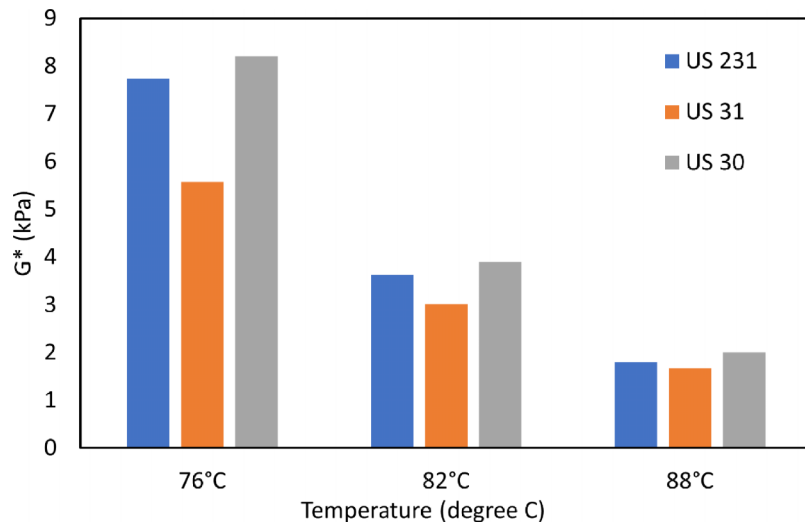
**Figure 4.14** G* results of the field core samples.

in 2018 and SP 5 mixtures were used for these sections. The original PG grade of US 231 was PG 70-22 and for US 31 and US 30, PG 76-22 was used. Though US 31 was constructed with PG 76-22, the G* results showed lower values than US 231 which was PG 70-22. From the Job Mix Formula (JMF) it was found that the binder replacement for US 31 is lower (22.7%) than for US 231 (24.3%). In addition, the field condition, climatic condition, and traffic volume have a signifi-cant impact on the field aging.

Also, the field aging was compared with lab aging. All the field cores are 4 years of age in the field. Here, the 5 days and 12 days of aging are conducted in the laboratory at 85°C. Previous research shows that 5-day lab aging at 85°C simulates approximately 7 years of field aging (Kim et al., 2021). Figure 4.15 shows that all 4 years of field aging are in between the unaged and 5 days of lab aging which is expected.

### 4.2.2 Frequency Sweep Test

The frequency sweep test was conducted in three different temperatures such as 10°C, 30°C, and 50°C at the frequency range of 0.1–25 Hz. G* master curve was prepared for both SP 5 and SP 4 extracted binder. Figure 4.16 shows the comparison of the G* master curve of SP 5 (64-22-9.5) vs. SP 4 (64-22-9.5). It is found that, in unaged conditions, the SP 5 and SP 4 curves show similar values. However, after aging the values are increasing and the SP 4 values are much higher than the SP 5.

Figure 4.17 shows the comparison of the G* master curve of SP 5 (64-22-12.5) vs. SP 4 (64-22-12.5). Similarly, it is found that after aging the values are increasing and the SP 4 values are much higher than the SP 5. Also, the increment rate is higher for SP 4 samples than the SP 5. These results also show a similar trend to the DSR test results.

Figure 4.18 shows the G* master curve of MS4 (PG 70-22) and EB4 (PG 76-22). It was found that MS4 shows higher G* values than EB4 though the PG grade is lower. The reason is the binder replacement percent for EB4 is only 18.5% whereas the binder replacement of MS4 is 23.6%. DSR test results also showed a similar trend for MS4 and EB4 comparison.

Figure 4.19 shows the G* master curve of field core samples. The original PG grade of US 231 was PG 70-22 and for US 31 and US 30, PG 76-22 was used. Though US 31 was constructed with PG 76-22, the G* results showed lower values than US 231 which was PG 70-22. From the JMF it was found that the binder replacement for US 31 is lower (22.7%) than US 231 (24.3%). DSR test results of field cores of Figure 4.14 show the same trend of G* values.

### 4.2.3 FTIR Test

FTIR is a technical method used to detect the infrared absorption of samples (Bowers et al., 2014). Spectral data is collected in a wide range of wave-lengths. The carbon and hydrogen content in the organic asphalt is over 90% (Asphalt Institute, 2003). In this study, the FTIR test was performed on unaged and aged samples to detect any change in the functional group due to the occurrence of oxidative aging. In this test, a vibrational Infrared (IR) light is passed through the sample in question. When the natural vibrational frequencies of a specific molecule match with the frequency of the IR radiation, the molecule absorbs the energy and increases the amplitude of vibrational motion is detected as a peak in the interferogram. In FTIR analysis, the natural vibrations of the covalent bonds among the molecules are exploited in any detection (Roy, 2021). As every type of bond has a different natural frequency of vibration, and two of the same type of bond in two different compounds are in two slightly different environments, therefore, no two molecules of the different structures have the same IR absorption pattern (Pavia et al., 2008). Figure 4.20 shows the FTIR results of the control asphalt binder.
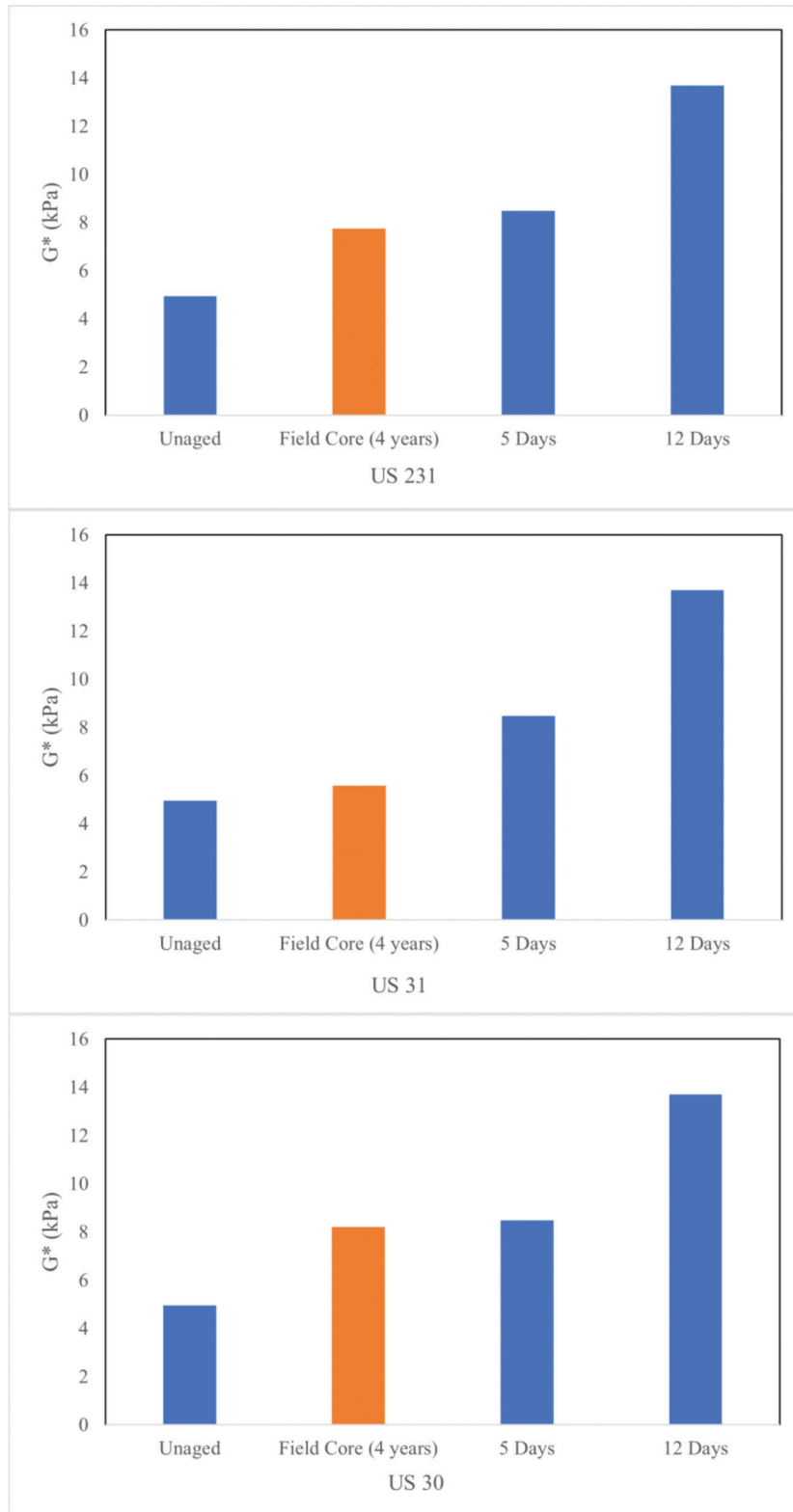
**Figure 4.15**   G* comparison of the field aging vs. lab aging.
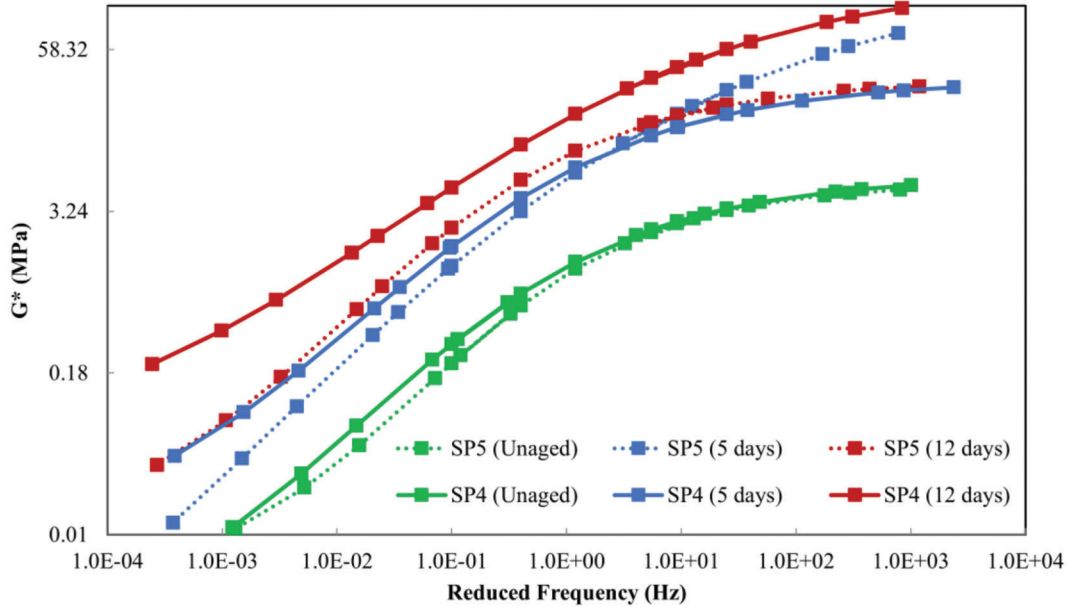
**Figure 4.16** Comparison of the G* master curve of SP 5 (64-22-9.5) vs. SP 4 (64-22-9.5).
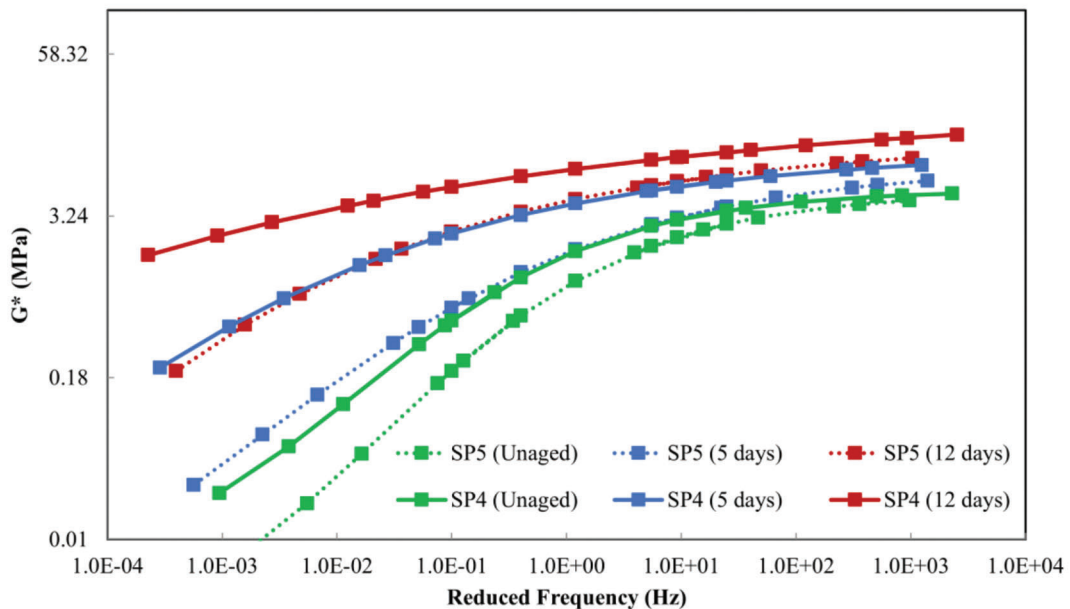


**Figure 4.17** Comparison of the G* master curve of SP 5 (64-22-12.5) vs. SP 4 (64-22-12.5).

During the asphalt aging process, the six functional groups (carboxylic acids, aldehydes, amides, anhydrides, esters, and ketones) containing the carbonyl group can be found in the asphalt binders based on the FTIR results. Based on the FTIR results, Figures 4.21 and 4.22 show the functional group peaks at different aging conditions, and due to aging the peak heights are increasing. In FTIR figures, the x-axis denotes the wavenumber (cm$^{-1}$), and the y-axis denotes the amount of absorbance, A (a.u.). The functional groups containing the carbonyl group in the asphalt binders can be also used to correlate to the oxidation extent of asphalt binders (Yao et al., 2015).

Figure 4.23 shows the comparison between the SP 5 and SP 4 FTIR results. The increments of the peaks are much higher for SP 4 due to aging. The peak increment for SP 5 from unaged to 5 days is 7.8%
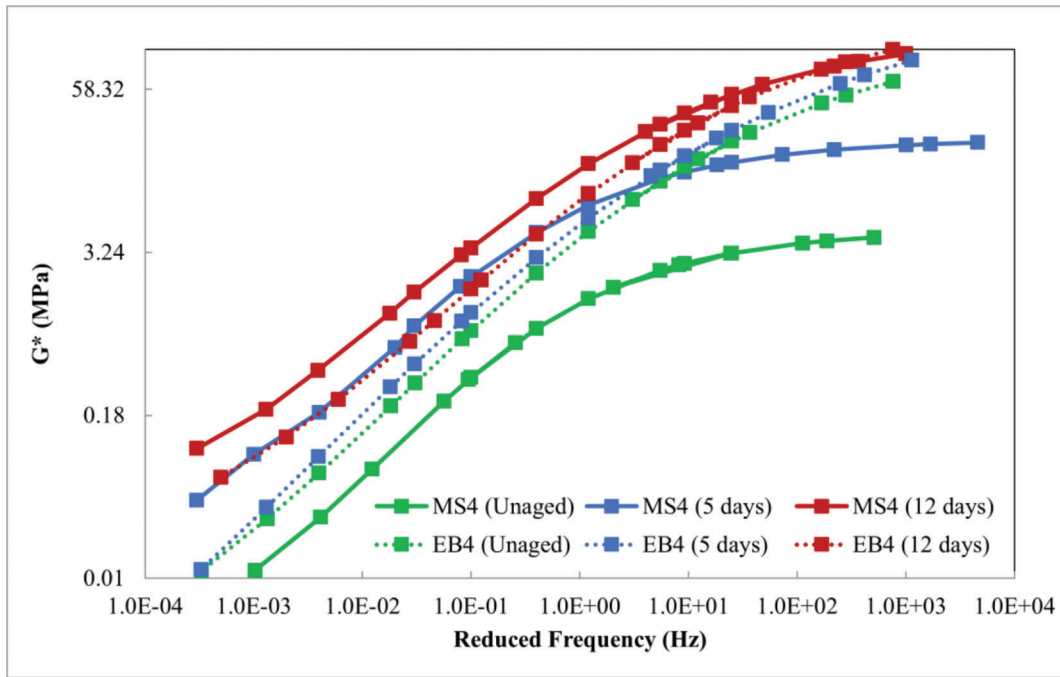
**Figure 4.18** G* master curve of MS4 and EB4.
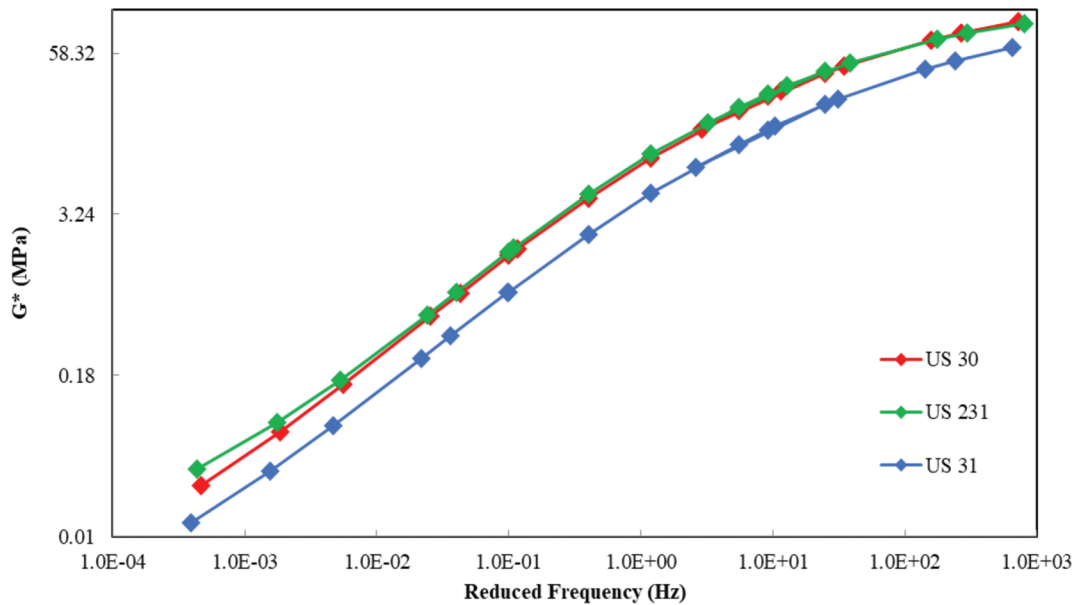


**Figure 4.19** G* master curve of field core samples.

whereas for SP 4, the increment is 24.9%. The peak increment for SP 5 from 5 days to 12 days is 19.6% whereas for SP 4, the increment is 30.7%. So, it can be deemed that higher air void of SP 4 leads to more aging and the functional group peaks are increasing to a higher extent than the SP 5 sample.
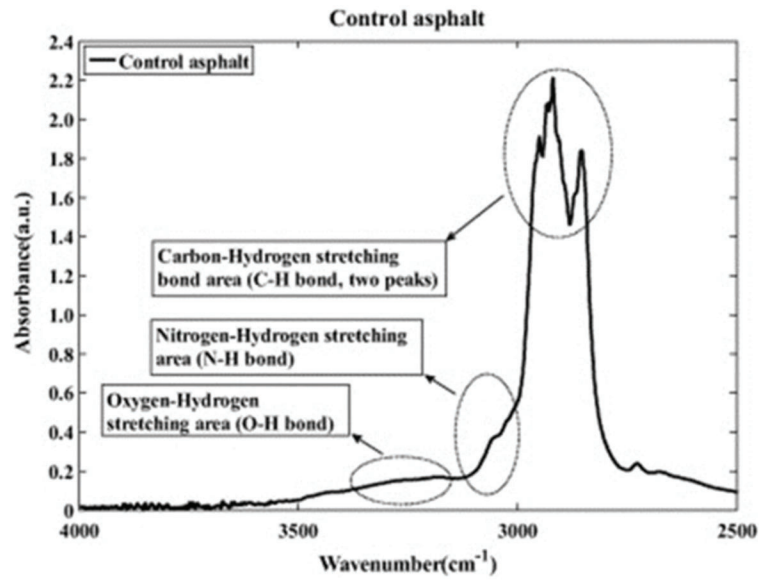
**Figure 4.20** FTIR results of control asphalt binder.
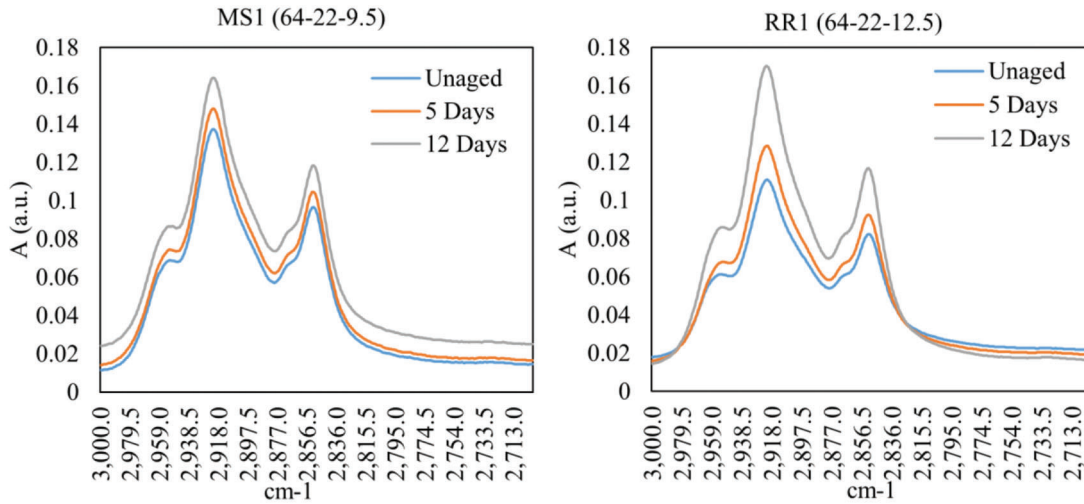


**Figure 4.21** FTIR results of MS1 and RR1 at different aging conditions.
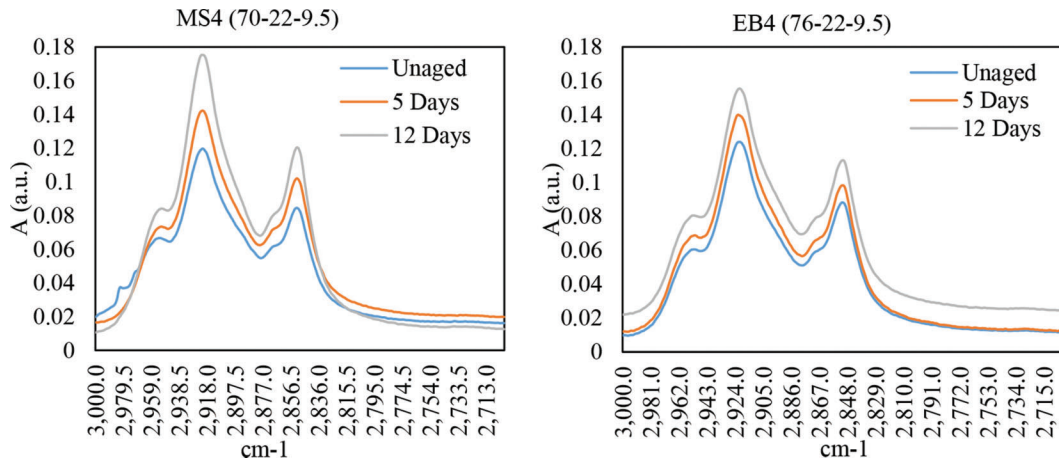


**Figure 4.22** FTIR results of MS4 and EB4 at different aging conditions.
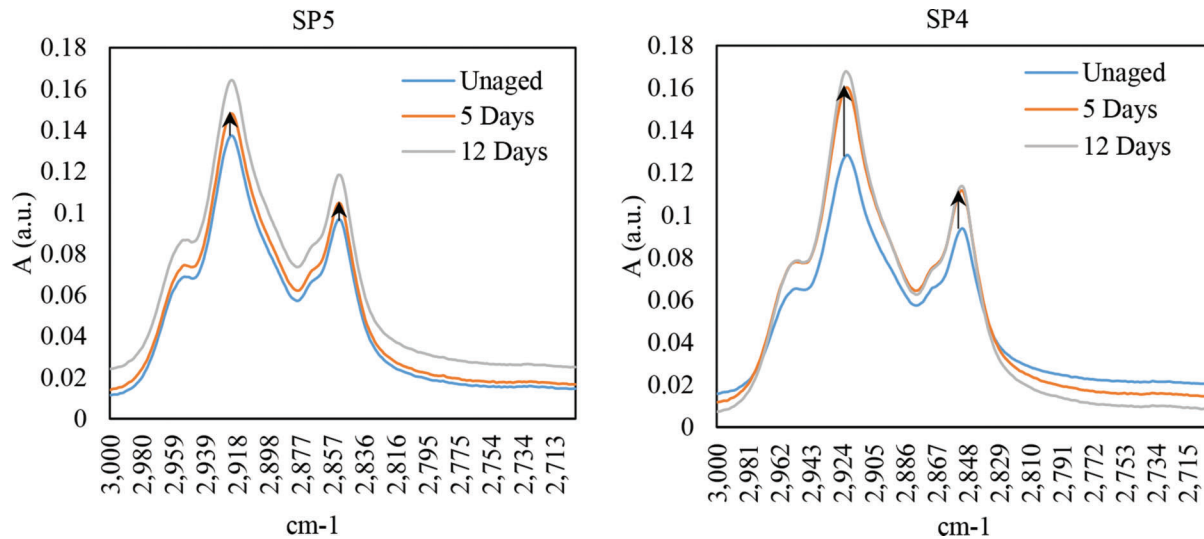
**Figure 4.23** FTIR comparisons of SP 5 (64-22-9.5) and SP 4 (64-22-9.5) at different aging conditions.

## 5. PAVEMENT PERFORMANCE PREDICTION USING PAVEMENT ME

The AASHTOWare Pavement ME has been used to provide the highway community with a practice tool for the design and analysis of new and rehabilitated pavement structures, based on mechanistic-empirical (M-E) principles (AASHTO, 2008). INDOT has been implementing MEPDG since January 1, 2009, with the INDOT Pavement ME input database developed by the Office of Research and Development and the Office of Pavement Engineering (Nantung et al., 2021). In this study, the AASHTOWare Pavement ME 2.3.1 version was used to simulate the pavement performance. Pavement ME uses a hierarchical level input system for most parameters related to traffic, material characteristics, and pavement conditions to allow a designer to better predict pavement responses given higher quality or project-specific data. The three levels and inputs used in this study are described in Table 5.1.

The pavement layer combinations selected for this study are shown in Table 5.2. The mixtures used in surface, intermediate, and base layers are the SP 5 mixtures. The laboratory test data were used for Level 1 input. The E* values at five different temperatures (-10°C, 4°C, 20°C, 40°C, and 55°C) and three different frequencies (0.1 Hz, 1 Hz, and 10 Hz) obtained from the dynamic modulus test were used as mixture input for Level 1. The G* values at three different temperatures along with phase angles obtained from the DRS test were used as binder input for Level 1. All the inputs (Level 1, Level 2, and Level 3) used in this study are given in the appendix section.

### 5.1 Prediction of Pavement Performance in Level 1 and Level 2

From Figure 5.1, it is found that Levels 1 and 2 are following a decreasing trend due to aging for bottom-up fatigue, top-down fatigue, and permanent deformation. However, the predicted values for bottom-up and top-down fatigue cracking are much higher for Level 2, which is not comparable with Level 1. For the thermal cracking, Level 1 is showing an increasing trend due to aging, but Level 2 is not following the same trend which means the Level 2 simulation will not provide us accurate distress prediction for thermal cracking. So, from Figure 5.1, it is evident that even though Level 2 follows a similar trend as Level 1, the distress values are much higher, and in some cases, Level 2 does not follow the trend. So, to find out the accurate pavement performance, Level 1 should be a good choice.

### 5.2 Prediction of Pavement Performance in Different Aging Conditions

The research team considered different aging conditions and ran the Pavement ME simulations for unaged, 5-day, and 12-day aged samples. Figure 5.2 shows the predicted distress values at different aging conditions. It is evident from Figure 5.2a, b, and d that top-down fatigue, bottom-up fatigue, and permanent deformation are decreasing due to aging. Because aging makes the binders stiffer, they are resistant to rutting (Ali et al., 2013; Bagchi et al., 2021; Zhang et al., 2018). However, the thermal cracking is increasing due to aging (Figure 5.2c). Because binder stiffness is a significant factor in thermal cracking. Softer asphalt binders and more angular aggregates improve the thermal cracking performance of an HMA (Aschenbrener, 1995). So, for 5-day and 12-day aged samples, the binders became stiffer, and increased thermal cracking was observed. Figure 5.1 does not show the Level 3 simulation results for 5 days and 12 days of aging because, for Level 3, PG grade is the input for Pavement ME. After aging, the PG grade would be higher (Xiao et al., 2013) than the original PG grade which is found in the job mix formula. So, it is not possible to input the PG grade after aging,

TABLE 5.1
**Pavement ME inputs**

| Level | Level of Reliability | Input |
|---|---|---|
| All Levels | | Asphalt martial properties: $P_{be}$, %AV<br>Climate: Indianapolis, 20 years of life<br>Traffic: 4,000 two-way AADTT, 4 lanes |
| Level 3 | Lowest | Aggregate gradation, PG Grade |
| Level 2 | Intermediate | G* and phase angle at multiple temps<br>Aggregate gradation |
| Level 1 | Highest | * values at multiple temperatures and frequencies<br>G* and phase angle at multiple temps |

TABLE 5.2
**Layer materials and thicknesses used for Pavement ME simulations**

| Layer Type | Material Type | Thickness (in) | Materials Used |
|---|---|---|---|
| Surface | Asphalt layer | 1.5 | MS1 (64-22-9.5), MS4 (70-22-9.5), and EB4 (76-22-9.5) |
| Intermediate | Asphalt layer | 2.5 | MS1 (64-22-9.5), MS4 (70-22-9.5), and RR1 (64-22-12.5) |
| Base | Asphalt layer | 6 | MS2 (64-22-19) |
| Non-Stabilized | Crushed gravel | 10 | – |
| Subgrade | A-1-a | Semi-infinite | – |
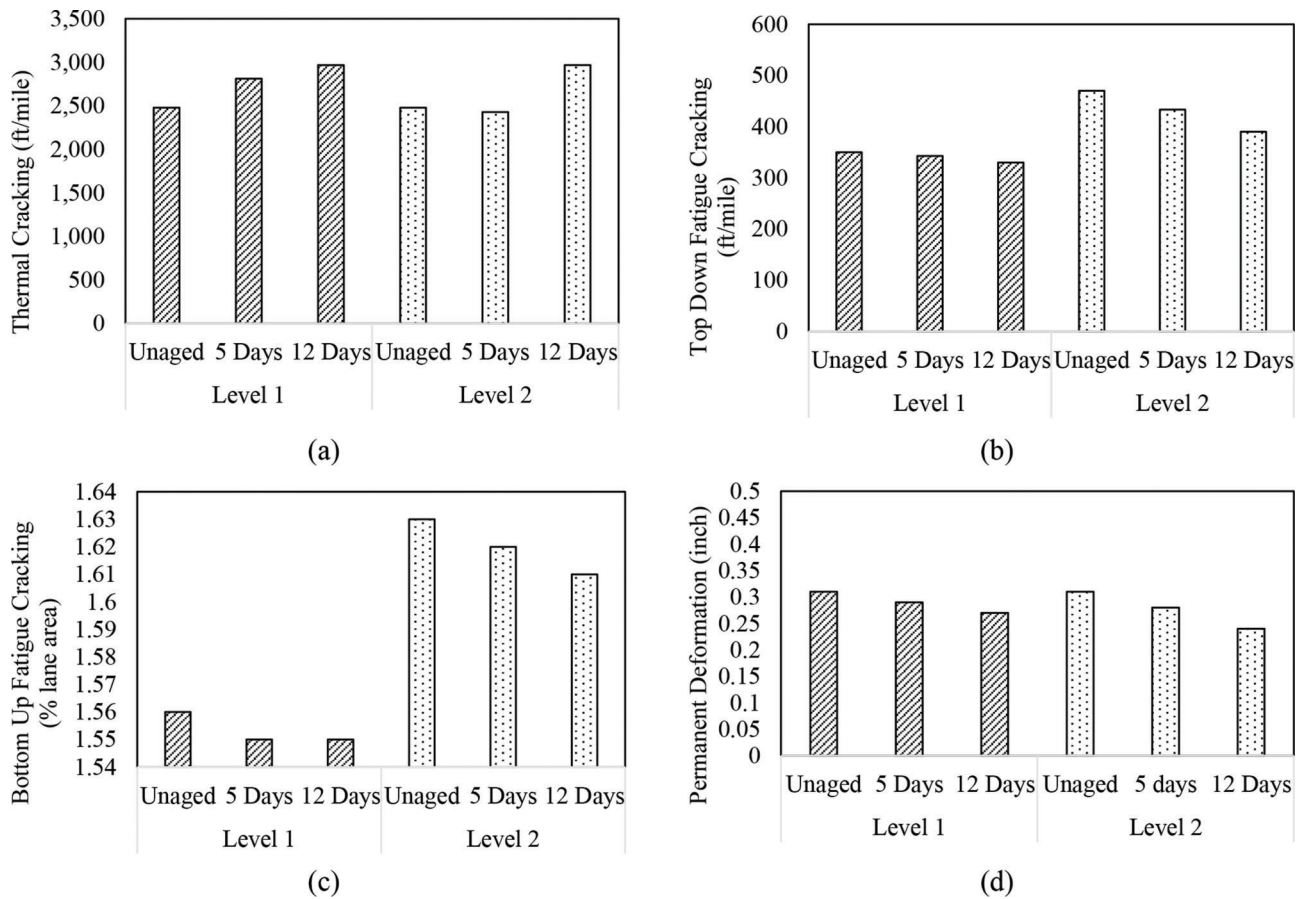


**Figure 5.1** Predicted distresses comparisons between Level 1 and Level 2.
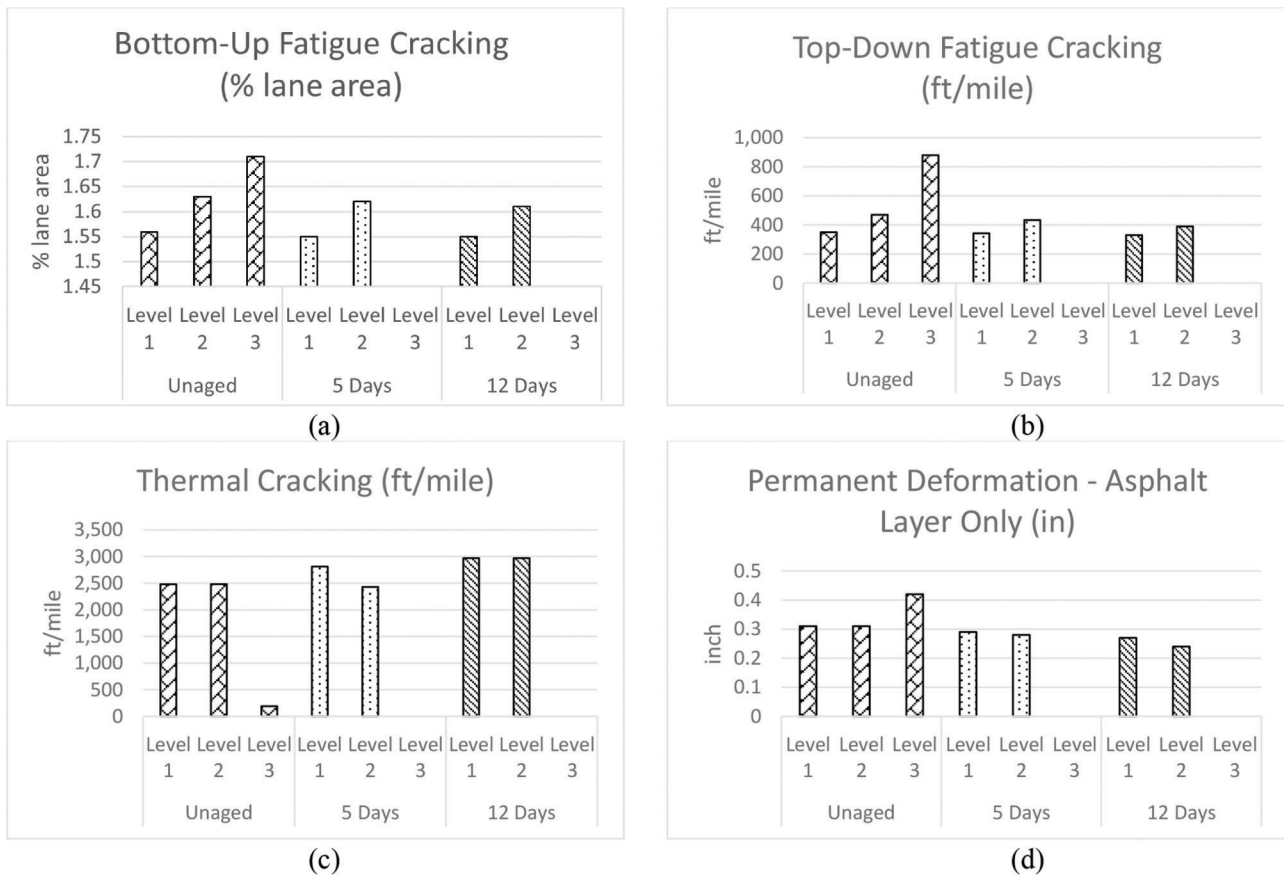
**Figure 5.2** Predicted distresses using different aging conditions.

TABLE 5.3
**SP 5 mixtures at different pavement layers used for Pavement ME simulations**

| Combination | Surface Layer Mixture | Intermediate Layer Mixture |
|---|---|---|
| No. 1 | MS1 (64-22-9.5) | MS1 (64-22-9.5) |
| No. 2 | MS1 (64-22-9.5) | RR1 (64-22-12.5) |
| No. 3 | MS4 (70-22-9.5) | RR1 (64-22-12.5) |
| No. 4 | MS4 (70-22-9.5) | MS1 (64-22-9.5) |
| No. 5 | EB4 (76-22-9.5) | MS1 (64-22-9.5) |

and for this reason, the research team is not showing the Level 3 simulation results for 5 days and 12 days.

### 5.3 Prediction of Pavement Performance of SP 5 Using Different Layer Thickness and Mixtures

In this project, Pavement ME simulations were conducted by using different pavement layer combinations by changing the mixture type of surface and intermediate layers. Figure 5.3 shows the predicted distresses of different layer combinations at Levels 1, 2, and 3. The list of layer combinations that were used for simulations is shown in Table 5.3. For these layer combinations, only the upper two layers' (surface and intermediate layer) materials were changed but the

other three layer's materials were the same as in Table 5.2. The combinations are denoted by Nos. 1 to 5.

Figure 5.3 shows the predicted distresses at Levels 1, 2, and 3 with different layer materials in unaged conditions. It is found that the distress values are decreasing due to using stiffer binders for all levels of simulations which is expected. Figure 5.3a, b showed the predicted values of the top-down and bottom-up fatigue cracking for Levels 1, 2, and 3. Level 3 shows much higher values compared to Levels 1 and 2. As Level 3 uses default input values, the distress prediction is not accurate and for top-down and bottom-up fatigue cracking, Level 3 is overestimating the fatigue cracking. Figure 5.3c shows the thermal cracking results and Level 3 underestimates the values compared to Levels 1 and 2. However, permanent deformation prediction does not follow any trend. For No. 1 and 2 where the layer material is a softer binder (PG 64-22), Levels 1 and 3 show similar results. However, using a stiffer binder, Levels 1 and 2 show similar results and Level 3 shows a much higher value. From the above discussion, it is evident that Level 3 simulation is underpredicting or overpredicting the distresses compared to Levels 1 and 2.

In addition, different base layer thickness was considered for simulation to find the impact of the base thickness. Figure 5.4 shows the predicted distresses
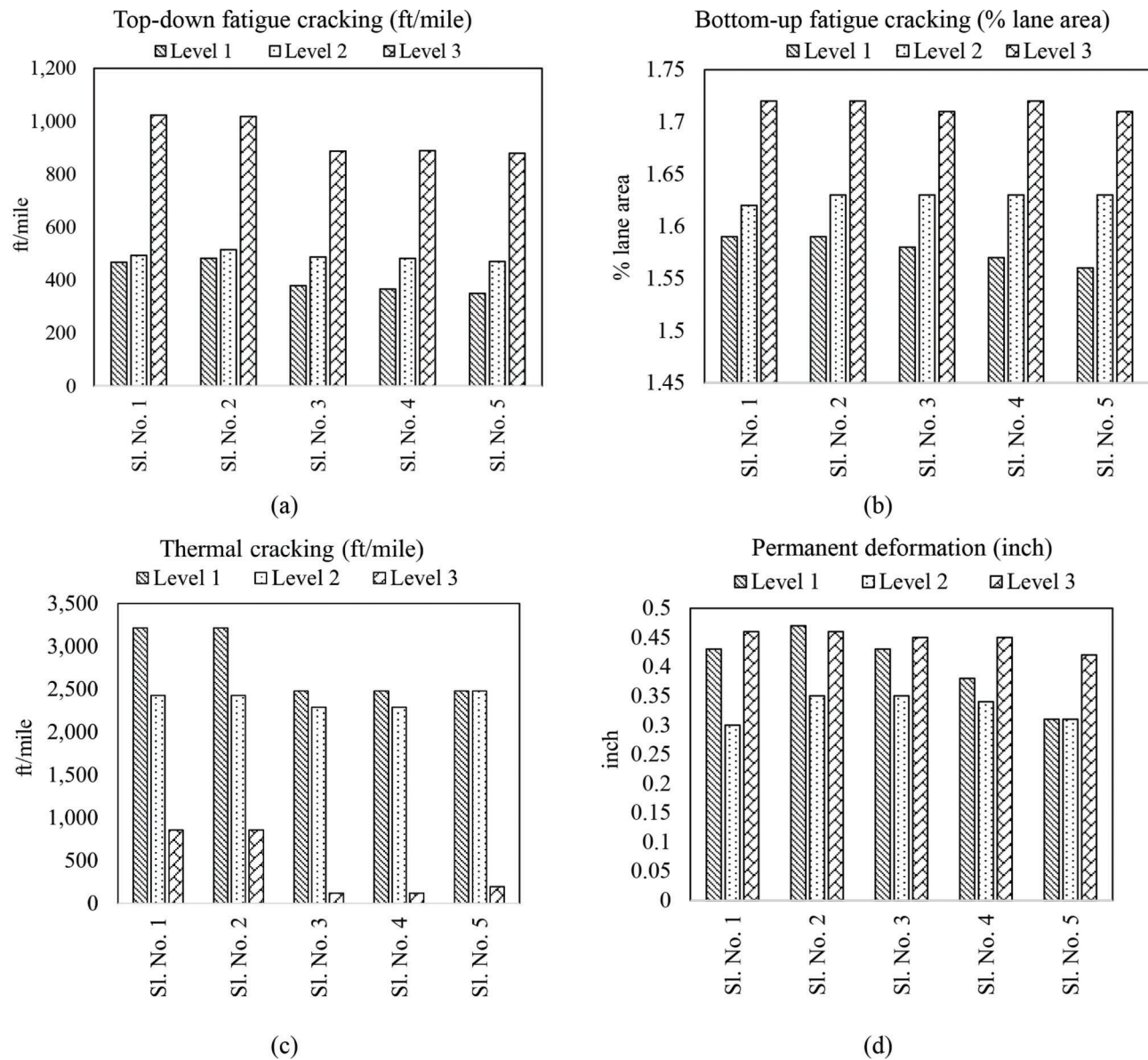
**Figure 5.3** Predicted distresses by using different SP 5 mixtures at different pavement layers.

using different base thicknesses. Three base thicknesses of 6 inches, 9 inches, and 12 inches were used to do the simulation and other properties remain the same. From Figure 5.4 it is evident that higher base thickness reduces the predicted distress values which is expected. Here, 9-inch and 12-inch base thicknesses show similar distress values whereas the 6-inch thickness shows much higher distress values.

## 5.4 Comparison of Performance Prediction Results for SP 5 and SP 4

In addition, the research team used the SP 4 mix to simulate the pavement performance and compared the distress values with the SP 5 simulation. For simulation, the same layer thickness was used for SP 5 and SP 4. Also, the same PG grade and NMAS were selected for SP 5 and SP 4. The Level 1 and Level 2 simulated distress values are shown in Table 5.4 and Table 5.5.

Based on the Table 5.4 and Table 5.5, SP 5 shows better performances than SP 4. Figure 5.5 and Figure 5.6 show a clearer understanding. Figure 5.5 and Figure 5.6 show the change in distress quantities (SP 5–SP 4) in Level 1 and Level 2. Higher distress indicates bad pavement performance, thus, if the (SP 5–SP 4) is negative, it means that SP 5 shows better performance than SP 4.

Figure 5.5 and Figure 5.6 show that most of the values are negative which means SP 5 provides better performance than SP 4. The reason is that SP 4 has a higher air void percentage and for this SP 4 undergoes more oxidative aging which leads to higher pavement distress. In addition, the consolidation effect under traffic loading would be another reason behind it.
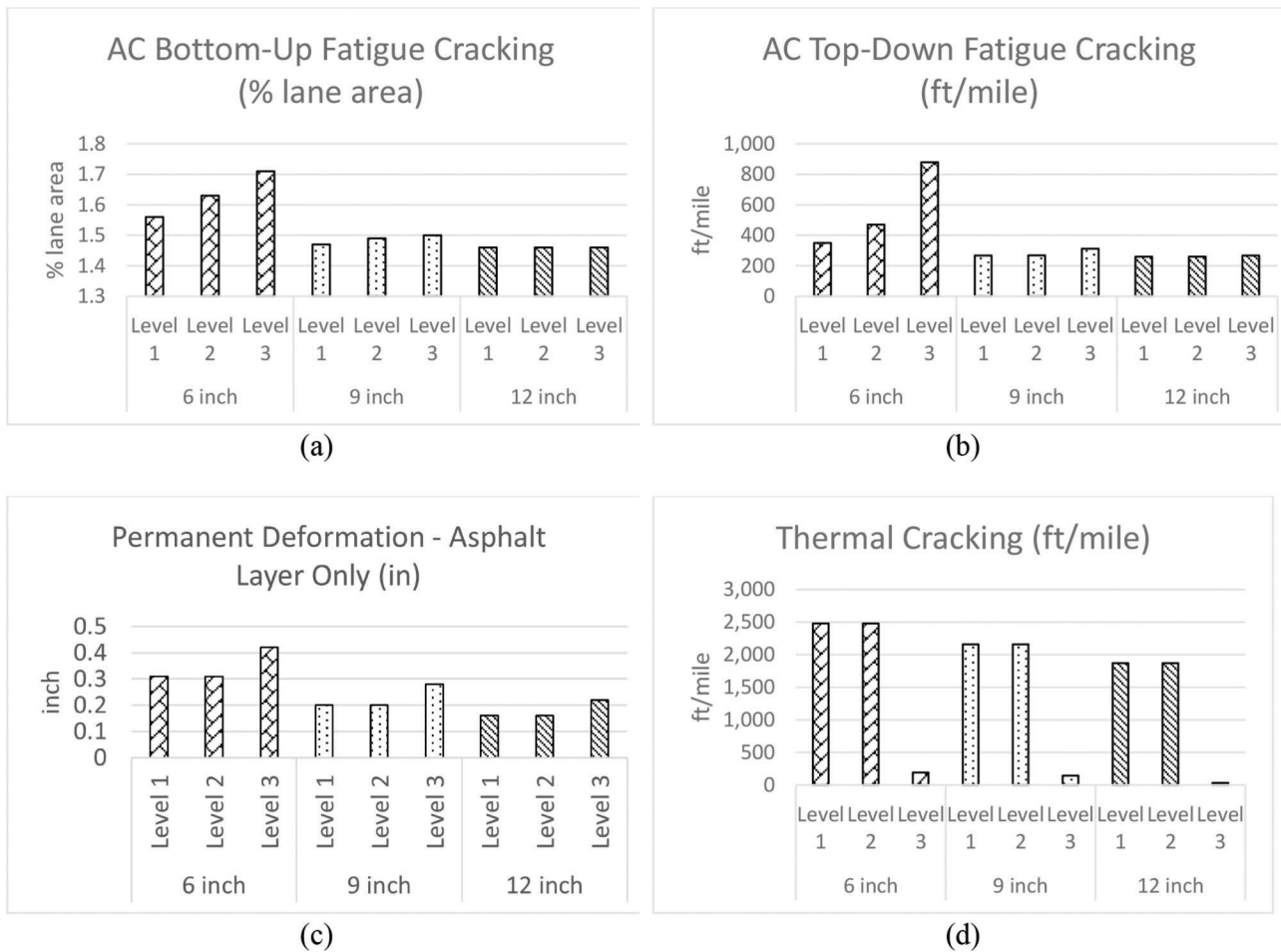
**Figure 5.4** Predicted distresses using different base thicknesses.

TABLE 5.4
**Comparison between SP 5 and SP 4 distress prediction in Level 1 design**

| Level 1 | Unaged | | 5 Days | | 12 Days | |
|---|---|---|---|---|---|---|
| Distress Type | SP 5 | SP 4 | SP 5 | SP 4 | SP 5 | SP 4 |
| Bottom-Up Fatigue Cracking (% lane area) | 1.59 | 1.59 | 1.57 | 1.59 | 1.57 | 1.58 |
| Thermal Cracking (ft/mile) | 3,213.25 | 3,008.82 | 2,429.85 | 2,842.46 | 2,648.61 | 3,088.89 |
| Top-Down Fatigue Cracking (ft/mile) | 467.41 | 705.93 | 402.75 | 676.65 | 387.07 | 594.18 |
| Permanent Deformation– Asphalt Layer Only (in.) | 0.43 | 0.45 | 0.36 | 0.43 | 0.33 | 0.37 |

## 5.5 Input Parameter Verification in Levels 1, 2, and 3

Based on the above discussion, it is evident that Levels 2 and 3 are not estimating the accurate pavement performance. In this study, the research team investigated the input parameters and analyzed the factors that are affecting the results. Figure 5.7 shows the mixture and binder inputs for Pavement ME in three different levels. For the input Level 1, the lab test results e.g., dynamic modulus of the mixture and the binder G* along with phase angle are used whereas Level 2 uses the aggregate gradation instead of dynamic

TABLE 5.5
**Comparison between SP 5 and SP 4 distress prediction in Level 2 design**

| Level 2 | Unaged | | 5 Days | | 12 Days | |
|---|---|---|---|---|---|---|
| Distress Type | SP 5 | SP 4 | SP 5 | SP 4 | SP 5 | SP 4 |
| Bottom-Up Fatigue Cracking (% lane area) | 1.62 | 1.63 | 1.63 | 1.97 | 1.62 | 1.62 |
| Thermal Cracking (ft/mile) | 2,425.85 | 3,088.89 | 2,427.24 | 2,842.46 | 2,425.85 | 3,211.26 |
| Top-Down Fatigue Cracking (ft/mile) | 493.34 | 799.98 | 494.23 | 922.06 | 463.78 | 695.76 |
| Permanent Deformation–Asphalt Layer Only (in.) | 0.3 | 0.33 | 0.31 | 0.33 | 0.28 | 0.28 |
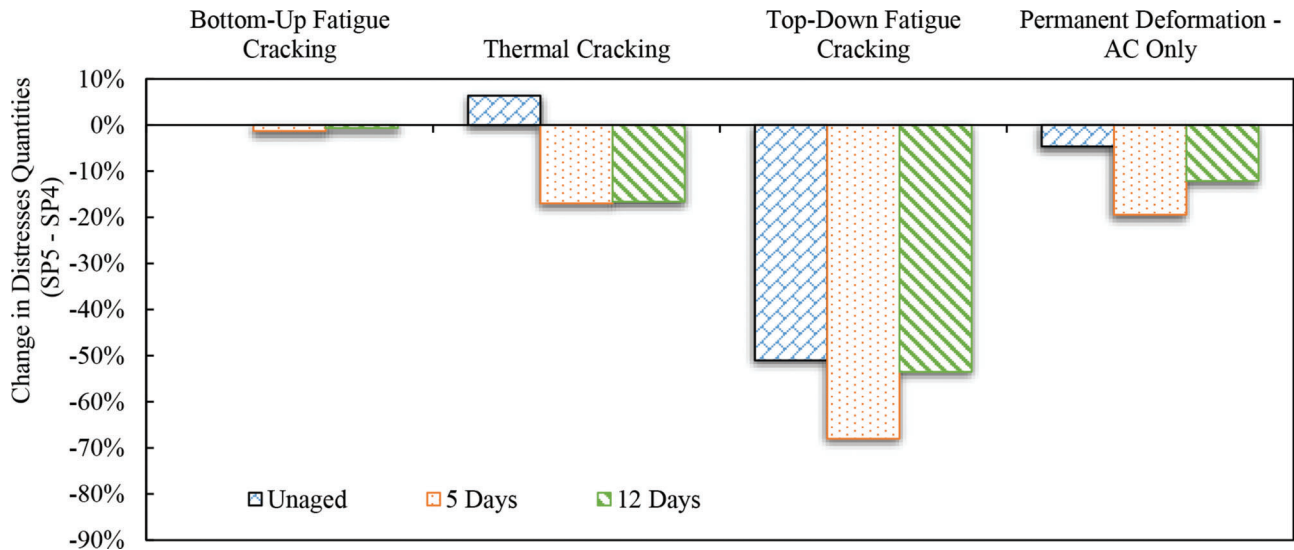


**Figure 5.5** Change in distress quantities of SP 5 vs. SP 4 in Level 1.



**Figure 5.6** Change in distress quantities of SP 5 vs. SP 4 in Level 2.

**Figure 5.7** Mixtures and binder inputs for Pavement ME in Levels 1, 2, and 3.
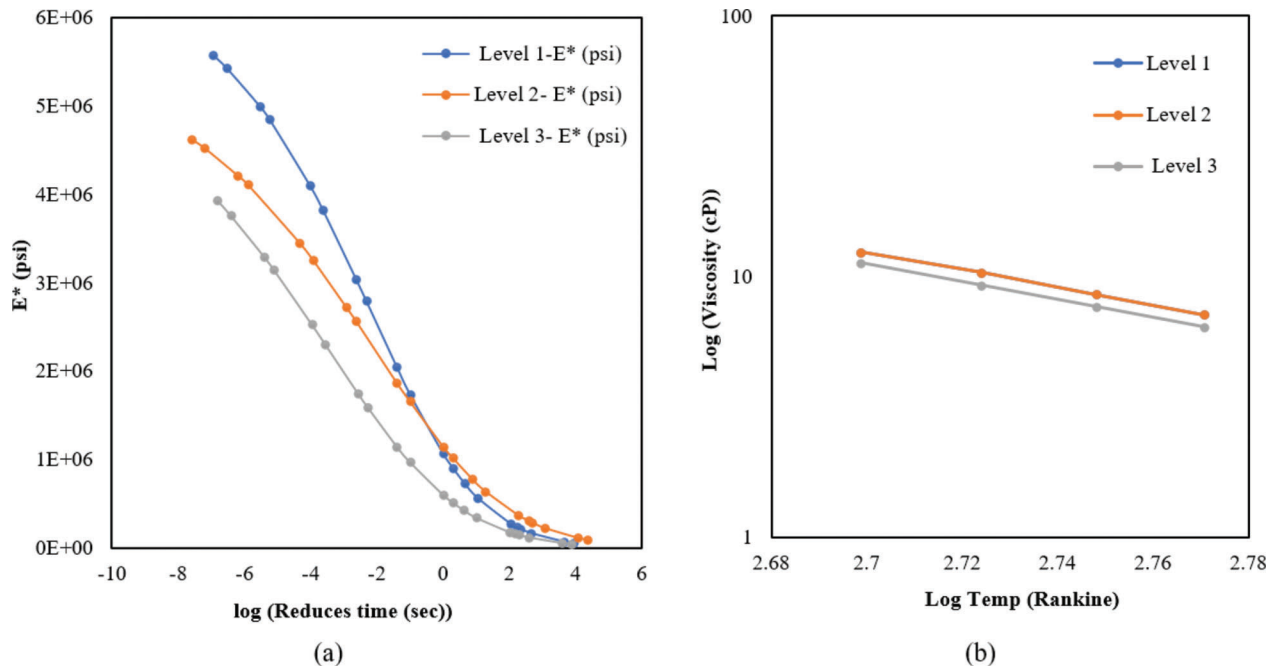


**Figure 5.8** Calculated E* and viscosity in Pavement ME based on Levels 1, 2, and 3 inputs.

modulus. But binder input remains the same for Level 2. However, Level 3 uses the aggregate gradation and the binder PG grade as input.

### 5.5.1 E* and Viscosity Prediction Based on Level Input Parameters

Based on these inputs, Pavement ME calculates the E* master curve and binder viscosity which is used for the simulation. Figure 5.8a shows the E* master curve for Levels 1, 2, and 3. Figure 5.8 shows that there is a huge difference in E* between the three levels. Level 1 E* represents the lab test results. However, Levels 2 and 3 show lower E* value, and Pavement ME either overestimates or underestimates the pavement distresses. Figure 5.8b shows the binder viscosity curve which is calculated based on the binder input. For Levels 1 and 2, the lab test results are used, so the viscosity curve is the same for these two. But the level

uses the PG grade, here PG grade is PG 70-22. In Level 3 simulation, Pavement ME uses the default viscosity values for PG 70-22, however, the binder used in the lab testing was more viscous which is represented by the DSR test result. Because, in the mixture, there is a certain percentage of RAP which is not considered for Level 3.

### 5.5.2 E* Prediction by Changing Air Void and Binder Content

In addition, the other input parameters such as air void, binder content, and PG grade were changed to find out the variation in the E* calculation. For Level 2 simulation, ±0.5% air void and ±1% binder content were changed and the calculated E* is shown in Figure 5.9. Similarly, for Level 3 simulation, ±0.5% air void and ±1% binder content were changed and the calculated E* is shown in Figure 5.10. For lowering
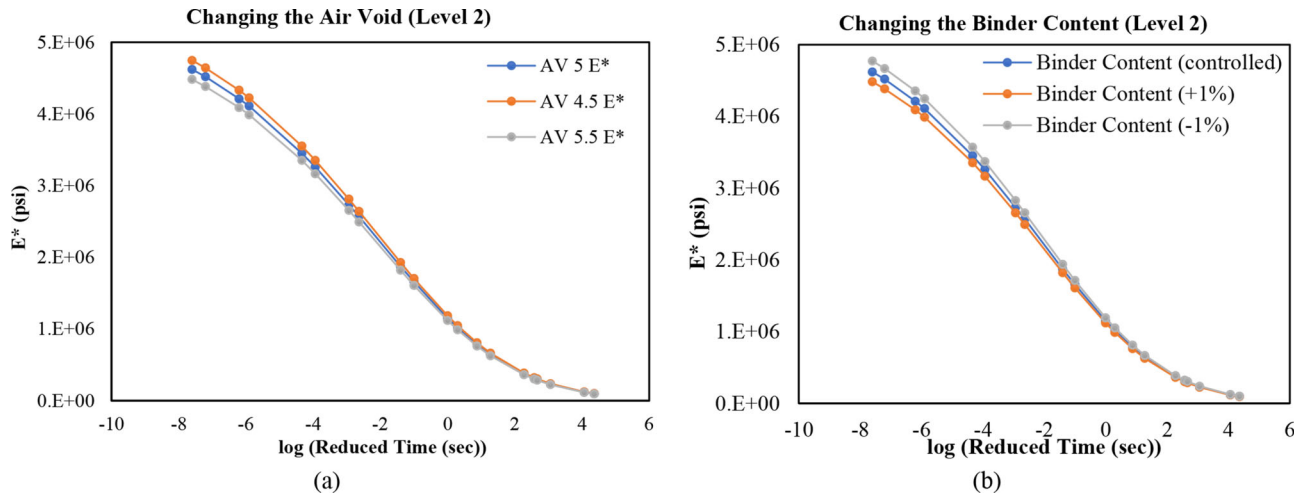
**Figure 5.9** Level 2 prediction by changing air void and binder content.
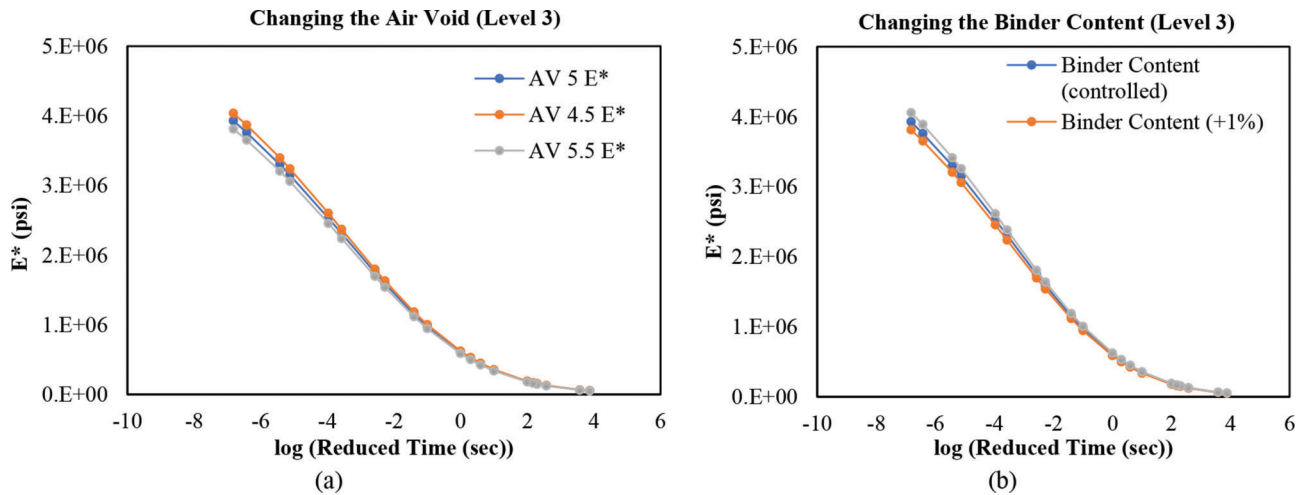


**Figure 5.10** Level 3 prediction by changing air void and binder content.

air void or binder content, the E* master curve shifted upward, and for increasing the air void or binder content, the E* master curve shifted downward, but the change amount is very little for all cases.

### 5.5.3 E* Prediction by Changing PG Grade

For Level 3 simulation, the PG grade was also changed one grade higher (PG 76-22) and lower (PG 64-22). Figure 5.11 shows the calculated E* and there is a significant difference due to the change in PG grade because it changed the viscosity curve.

Also, a similar change in air void and binder content was performed for Level 1, and there was no change at all. Because Level 1 uses the lab test results of dynamic modulus and binder G* and phase angle.

### 5.6 Comparison of Predicted E* and Lab-Measured E*

To compare the Pavement ME predicted E* and lab-measured E*, field core samples were collected from three different locations, each pavement having been in service for 4 years. The dynamic modulus test was conducted on the surface layer of the field cores. The field core details are shown in Table 5.6.

The Pavement ME simulation output file provides the predicted dynamic modulus in different temperature ranges. To compare the predicted values with lab-measured values, there are a few conversions such as Pavement ME loading time calculation and conversion from the time domain to frequency domain were conducted. The frequency of loading in HMA because of a moving load is determined based on Equation 1 in Table 5.7. By using Equation 1, the effective length can be related to the duration of the vertical stress pulse at any depth within the pavement system. To calculate the effective length at a specified depth, Pavement ME uses Odemark's method of thickness equivalency to transform the pavement structure into a single subgrade layer system. In addition, the stress distribution for a given subgrade soil is assumed to be at 45°. For the transformed section, the depth of the frequency
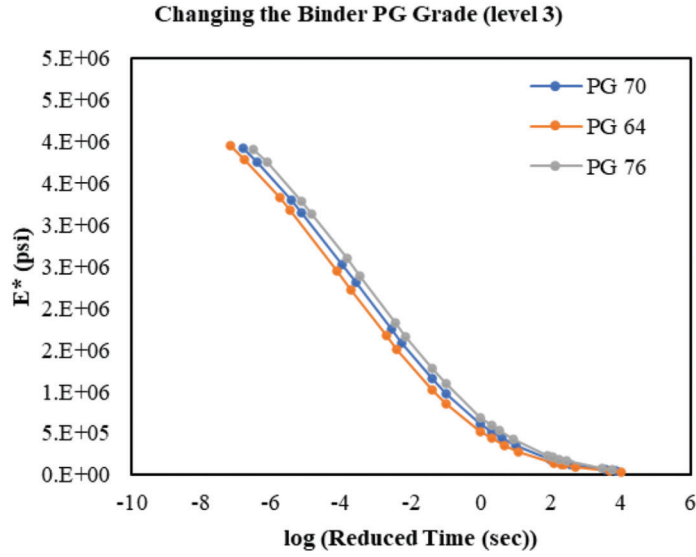
**Figure 5.11**  Level 3 prediction by changing PG grade.

TABLE 5.6
**Collected field core samples**

| Field Core | Construction Time | Original Grade | Binder Replacement (%) |
|---|---|---|---|
| US 231 | June 27 to September 17, 2018 | PG 70-22 | 24.3 |
| US 31 | September 4 to December 2, 2018 | PG 76-22 | 22.7 |
| US 30 | June 6 to July 19, 2018 | PG 76-22 | 19.7 |

TABLE 5.7
**Equations used for comparison of predicted E\* and lab-measured E\* (Al-Qadi et al., 2008)**

| | | |
|---|---|---|
| $t = \dfrac{L_{eff}}{17.6 v_s}$ | t = time of loading (s)<br>$L_{eff}$ = effective length (in)<br>$V_s$ = vehicle speed (mph) | Eq. 1 |
| $Z_{eff} = \sum_{i=1}^{n-1} \left( h_1 \sqrt[3]{\dfrac{E_i}{E_{SG}}} \right) + h_n \sqrt[3]{\dfrac{E_n}{E_{SG}}}$ | $Z_{eff}$ = effective depth<br>$h_n$ = thickness of the layer of interest<br>$E_{SG}$ = subgrade modulus of elasticity<br>$E_n$ = modulus of elasticity of the layer of interest | Eq. 2 |
| $L_{eff} = 2 * (a_c + Z_{eff})$ | $a_c = \dfrac{L}{2}$<br><br>$L = \sqrt{\dfrac{Contact\ Area}{0.5227}}$<br><br>$Contact\ Area = \dfrac{Load}{Tire\ Pressure}$<br>$L_{eff}$ = effective length (in)<br>$Z_{eff}$ = effective depth | Eq. 3 |
| $f = \dfrac{1}{2\pi t}$ | f = frequency (Hz)<br>t = time of loading (s) | Eq. 4 |

calculation changes and is calculated by using Equation 2. The effective length is calculated by using Equation 3. In MEPDG, the conversion from the time (t) domain to the frequency (f) domain (in hertz) is based on Equation 4.

By using the above equations, the frequency was found to be 1 Hz. Pavement ME shows the predicted dynamic modulus values for every month. For calculations, the dynamic modulus values are grouped as seasons as shown in Table 5.8.

For a better understanding, the predicted dynamic modulus values are plotted in Figure 5.12.

To compare these predicted values with field cores, the core sample with the same PG grade was selected

TABLE 5.8
**Predicted dynamic modulus in Pavement ME in different seasons after 4 years of construction**

| | Predicted Dynamic Modulus After 4 Years (psi) | | | | |
| | Temperature Range (1 means lower temperature and 5 means higher temperature) | | | | |
| Seasons | 1 | 2 | 3 | 4 | 5 |
|---|---|---|---|---|---|
| Dec-Jan-Feb | 4,032,580 | 4,032,580 | 4,032,580 | 4,032,580 | 4,032,580 |
| Mar-Apr-May | 4,032,580 | 3,929,790 | 3,633,330 | 3,251,093 | 2,581,763 |
| June-July-Aug | 2,613,856 | 2,005,340 | 1,609,183 | 1,211,490 | 858,615 |
| Sep-Oct-Nov | 4,032,580 | 3,474,160 | 3,066,016 | 2,755,053 | 2,213,153 |
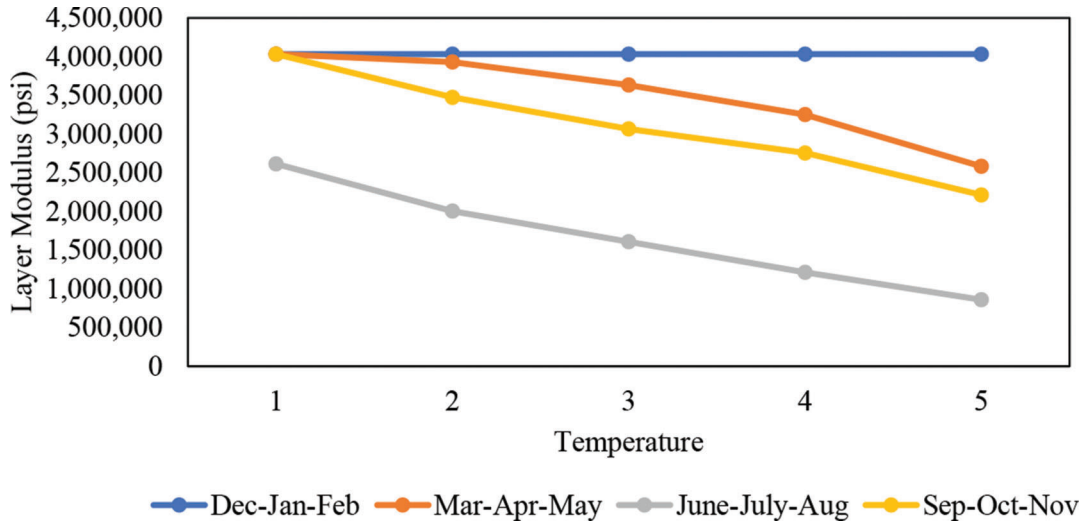


**Figure 5.12** Predicted dynamic modulus in Pavement ME at different temperatures after 4 years.

TABLE 5.9
**Lab measured dynamic modulus of US 231 field core**

| Field Core: US 231 | Dynamic Modulus (psi) | | |
| Temperature (°C) | 0.1 Hz | 1 Hz | 10 Hz |
|---|---|---|---|
| 4 | 1,836,143.178 | **2,376,604.482** | 2,887,747.054 |
| 10 | 1,300,507.315 | **1,850,378.251** | 2,390,229.262 |
| 20 | 589,046.5245 | **1,042,004.221** | 1,579,290.699 |
| 40 | 79,076.66254 | **191,259.7999** | 421,591.7862 |
| 55 | 20,969.15754 | **53,305.3408** | 132,116.7405 |

Note: Testing data at 1 Hz (bolded numbers) is comparable to dynamic modulus by Pavement ME.

and the lab-measured dynamic modulus values are shown in Table 5.9.

So, the lab-measured dynamic modulus at 1 Hz at different temperatures are much lower than those predicted by the Pavement ME. Similar results were also found for field cores on US 30 and US 31. So, Pavement ME is overpredicting the dynamic modulus values compared to the original lab test results. Previous researchers also found that Pavement ME is overpredicting the dynamic modulus (Al-Qadi et al., 2008).

## 6. SUMMARY AND RECOMMENDATIONS

In order to evaluate the Superpave 5 mixtures and compare the difference in performance due to the aging effect between Superpave 5 and conventional Superpave 4, several mixture tests and binder tests were conducted. Three aging levels (unaged, 5 days aging, and 12 days aging) were set for the lab-prepared samples. The performance prediction results using Pavement ME for Superpave 5-designed and conventional Superpave-designed mixtures were compared to identify performance enhancements gained by using Superpave 5-designed asphalt mixtures. Also, the research team evaluated the accuracy of Pavement ME's three analysis levels to predict the pavement performance of the SP 5 mixture. The study findings are summarized as follows.

- Dynamic modulus test results showed that SP 5, with lower air voids, can slow down aging compared to SP 4. Additionally, it was shown that the modified high-viscosity asphalt binder has a lesser effect on aging than the normal asphalt binder.
- The HWTT results showed that the initial rutting of SP 5 was smaller than that of SP 4 due to low air voids. However, due to the greater increase in stiffness due to aging in SP 4, the rut depth after aging showed similar values in both mixtures.

- The cyclic fatigue index parameter, $S_{app}$, obtained through a fatigue test, showed that the decrease in cracking resistance due to aging of SP 5 was significantly lower than that of SP 4, confirming that the SP 5 mixture has a benefit in fatigue cracking resistance.
- DSR test results indicate that the G* value is increasing due to aging for both SP 5 and SP 4 samples. However, SP 4 shows a higher percentage of increment of G* than SP 5. G* master curve from the frequency sweep test also shows a similar trend.
- The FTIR test results show that the increments of the functional group peaks are much higher for SP 4 due to aging. The peak increment for SP 5 from unaged to 5 days is 7.8% whereas for SP 4, the increment is 24.9%. The peak increment for SP 5 from 5 days to 12 days is 19.6% whereas for SP 4, the increment is 30.7%. So, it can be deemed that higher air void of SP 4 leads to more aging and the functional group peaks are increasing to a higher extent than the SP 5 sample.
- Pavement-ME simulations have shown that there is a significant difference between Level 1, Level 2, and Level 3 thermal cracking, rutting, bottom-up fatigue cracking, and top-down fatigue cracking.
- Levels 2 and 3 underestimated the benefits of SP 5 due to the use of default values calibrated based on SP 4, while Level 1 might capture the benefits of SP 5 using lab test results.
- Superpave 4 mixtures indicated the greater permanent deformation than SP 5 mixtures due to higher air voids and consolidation effect under the traffic loading.
- Superpave 5 (SP 5) mixtures showed the better resistance against cracking performance based on the Pavement-ME simulation results due to higher in-place density and lower oxidative aging.
- Change in air voids and change in binder content do not have a significant impact on calculating the input E* in Pavement ME. However, changing the PG grade has a significant impact on calculating the input E* in Pavement ME.
- Pavement ME is overpredicting the long-term dynamic modulus values compared to the original lab test results even in Level 1 simulation.
- To capture the benefit of SP 5 pavement design, the Level 1 inputs (lab test results) are recommended for the Pavement ME also the local calibration factors need to be calibrated based on SP 5.

# REFERENCES

AASHTO. (2008). *Mechanistic-empirical pavement design guide: A manual of practice*. American Association of State and Highway Transportation Officials.

AASHTO. (2010). *AASHTO T 315: Standard method of test for determining the rheological properties of asphalt binder using a dynamic shear rheometer (DSR)*. American Association of State and Highway Transportation Officials.

AASHTO. (2013). *AASHTO M 323-13: Standard specification for superpave volumetric mix design*. American Association of State Highway and Transportation Officials.

AASHTO. (2019). *AASHTO T 324-19: Standard method of test for Hamburg wheel-track testing of compacted asphalt mixtures*. American Association of State and Highway Transportation Officials.

Ali, U. M. (2019). *Evaluating the cracking resistance of a Superpave 5 mix and a conventional Superpave mix using the Illinois Flexibility Index Test*. University of Illinois, IL.

Ali, A. H., Mashaan, N. S., & Karim, M. R. (2013). Investigations of physical and rheological properties of aged rubberised bitumen. *Advances in Materials Science and Engineering, 2013*, 239036.

Al-Qadi, I. L., Elseifi, M. A., Yoo, P. J., Dessouky, S. H., Gibson, N., Harman, T., D'Angelo, J., & Petros, K. (2008). Accuracy of current complex modulus selection procedure from vehicular load pulse: NCHRP project 1-37a mechanistic-empirical pavement design guide. *Transportation Research Record*, *2087*(1), 81–90.

Aschenbrener, T. (1995). *Investigation of low temperature thermal cracking in hot mix asphalt* (Report. No. CDOT-DTD-R-95-7). Colorado Department of Transportation.

Asphalt Institute. (2003). *Superpave performance graded asphalt binder specification and testing* (Superpave Series No. 1, 3rd ed.).

ASTM. (2011). *ASTM D2172: Standard test methods for quantitative extraction of bitumen from bituminous paving mixtures*. ASTM International.

ASTM. (2012). *ASTM D5404: Standard practice for recovery of asphalt from solution using the rotary evaporator*. ASTM International.

Bagchi, T., Hossain, Z., Ziaur Rahaman, M., & Baumgardner, G. (2021). Comparing micro-and macro-level rheological properties of polymeric and reclaimed asphalt pavement-modified asphalt binders. *Transportation Research Record*, *2675*(12), 247–263.

Bowers, B. F., Huang, B., Shu, X., & Miller, B. C. (2014). Investigation of reclaimed asphalt pavement blending efficiency through GPC and FTIR. *Construction and Building Materials*, *50*, 517–523.

Esfandiarpour, S., Ahammed, M. A., Shalaby, A., Liske, T., & Kass, S. (2013, September). *Sensitivity of pavement ME design predicted distresses to asphalt materials inputs* [Conference presentation]. 2013 Conference and Exhibition of the Transportation Association of Canada-Transportation: Better-Faster-Safer (TAC/ATC'13), Winnipeg, Manitoba, Canada.

Etheridge, R. A., Wang, Y. D., Kim, S. S., & Kim, Y. R. (2019). Evaluation of fatigue cracking resistance of asphalt mixture using apparent damage capacity. *Journal of Materials in Civil Engineering*, *31*(11), 04019257-1–04019 257-12.

Haddock, J. E., Rahbar-Rastegar, R., Pouranian, M. R., Montoya, M., & Patel, H. (2020). *Implementing the Superpave 5 asphalt mixture design method in Indiana* (Joint Transportation Research Program Publication No. FHWA/IN/JTRP-2020/12). West Lafayette, IN: Purdue University. https://doi.org/10.5703/1288284317127

Hekmatfar, A., McDaniel, R. S., Shah, A., & Haddock, J. E. (2015). *Optimizing laboratory mixture design as it relates to field compaction to improve asphalt mixture durability* (Joint Transportation Research Program Publication No. FHWA/IN/JTRP-2015/25). West Lafayette, IN: Purdue University. https://doi.org/10.5703/1288284316010

Hossain, Z., Elsayed, A., Bagchi, T., & Roy, S. (2020). *Assessment of compatibility of mineral aggregates and binders used in highway construction and maintenance* projects (Tran-SET Project: 19BASU02). https://repository.lsu.edu/transet_pubs/72

Huber, G., Wielinski, J., Campbell, C., Padgett, J., Rowe, G., Beeson, M., & Cho, S. (2019). SuperPave5: Relationship of

in-place air voids and asphalt binder aging. *Journal of Association of Asphalt Paving Technologist*s, *88*, 183–215.

Kim, Y. R., Castorena, C., Elwardany, M. D., Rad, F. Y., Underwood, S., Gundha, A., Gudipudi, P., Farrar, M. J., & Glaser, R. R. (2021). *NCHRP Research Report 973: Long-term aging of asphalt mixtures for performance testing and prediction: Phase III results* (NCHRP Project 09-54). National Cooperative Highway Research Program. https://doi.org/10.17226/26133

Montoya, M. A., Pouranian, M. R., & Haddock, J. E. (2018). Increasing asphalt pavement density through mixture design: A field project. In *Asphalt Paving Technology: Association of Asphalt Paving Technologists-Proceedings of the Technical Sessions*, *87*, 1–29.

Moutier, F. (1982). Prevision de la compactabilite des enrobes bitumineux a l'aide de la presse a cisaillement giratoire (PCG). *Bull Liaison Lab Ponts Chauss*, (121), 29–40.

Nantung, T. E., Lee, J., Haddock, J. E., Pouranian, M. R., Alvarez, D. B., Jeon, J., Shin, B., & Becker, P. J. (2021). *Structural evaluation of full-depth flexible pavement using APT* (Joint Transportation Research Program Publication No. FHWA/IN/JTRP-2021/17). West Lafayette, IN: Purdue University. https://doi.org/10.5703/1288284317319

Pavia, D. L., Lampman, G. M., Kriz, G. S., & Vyvyan, J. A. (2008). *Introduction to spectroscopy* (5th ed.). Cengage Learning.

Roy, S. (2021). *Efficacy of softener for enhancing fatigue and low-temperature performance of asphalt binders with high RAP*. Arkansas State University.

Valentová, T., Altman, J., & Valentin, J. (2016). Impact of asphalt ageing on the activity of adhesion promoters and the moisture susceptibility. *Transportation Research Procedia*, *14*, 768–777.

Wang, Y. D., & Kim, Y. R. (2017). Development of a pseudo strain energy-based fatigue failure criterion for asphalt mixtures. *International Journal of Pavement Engineering*, *20*(10), 1182–1192. http://dx.doi.org/10.1080/10298436.2017.1394100

Watson, D. E., Brown, E. R., & Moore, J. R. (2005). Comparison of Superpave and Marshall mix performance in Alabama. *Transportation Research Record*, *1929*(1), 133–140.

Xiao, F., Chen, M., Wu, S., & Amirkhanian, S. N. (2013). A long-term ultraviolet aging effect on rheology of WMA binders. *International Journal of Pavement Research and Technology*, *6*(5), 496–504.

Yan, T., Marasteanu, M., Le, J.-L., Turos, M., & Cash, K. (2022, June). *Development of superpave 5 asphalt mix designs for Minnesota pavements* (MnDOT 2022-18). Minnesota Department of Transportation.

Yao, H., Dai, Q., & You, Z. (2015). Fourier transform infrared spectroscopy characterization of aging-related properties of original and nano-modified asphalt binders. *Construction and Building Materials*, *101*(Part 1), 1078–1087.

Zhang, H., Chen, Z., Xu, G., & Shi, C. (2018). Evaluation of aging behaviors of asphalt binders through different rheological indices. *Fuel*, *221*, 78–88.

Zhang, R., Sias, J. E., Dave, E. V. (2020). Evaluation of the cracking and aging susceptibility of asphalt mixtures using viscoelastic properties and master curve parameters. *Journal of Traffic and Transportation Engineering*, *9*(1), 106–119.

APPENDICES

**Appendix A. Pavement ME Input Parameter**

# APPENDIX A. PAVEMENT ME INPUT PARAMETER

**MS1-Unaged Inputs for Pavement ME:**

Table A.1 Mixture inputs for MS1-unaged

| Binder | | NAMS | $P_{be}$ (weight) | $G_{mb}$ | $P_{be}$ (volume) | $P_b$ (%) |
|---|---|---|---|---|---|---|
| MS1 Unaged | PG 64-22 | 9.5 | 4.9 | 2.319 | 11.4 | 6.4 |

Table A.2 Binder inputs (DSR results) for MS1-unaged

| Binder DSR Test | | | | |
|---|---|---|---|---|
| Temp (°C) | Temp (°F) | Binder G* (kPa) | Phase Angle (degrees) | Binder G* (Pa) |
| 70 | 158 | 7.14 | 80.3 | 7,140 |
| 76 | 168.8 | 2.87 | 82.8 | 2,870 |
| 82 | 179.6 | 1.39 | 84.8 | 1,390 |

Table A.3 Dynamic modulus inputs for MS1-unaged

| Mix Dynamic Modulus (psi) | | | | |
|---|---|---|---|---|
| Temp (°C) | Temp (°F) | 0.1 Hz | 1 Hz | 10 Hz |
| -10 | 14 | 2,529,671 | 2,999,405 | 3,444,234 |
| 4 | 39.2 | 1,377,419 | 1,873,788 | 2,365,059 |
| 20 | 68 | 406,783 | 758,515 | 1,211,631 |
| 40 | 104 | 54,105 | 132,445 | 299,148 |
| 55 | 131 | 13,953 | 35,690 | 89,296 |

Table A.4 Percent passing in different sieve sizes for MS1-unaged

| Sieve Size | % Passing |
|---|---|
| 3/4 | 100 |
| 3/8 | 94.8 |
| No 4 | 66.9 |
| No 200 | 5.6 |

**MS1-5 Days Inputs for Pavement ME:**

Table A.5 Mixture inputs for MS1-5 days

| Binder | | NAMS | $P_{be}$ (weight) | $G_{mb}$ | $P_{be}$ (volume) | $P_b$ (%) |
|---|---|---|---|---|---|---|
| MS1-5 Days | PG 64-22 | 9.5 | 4.9 | 2.34 | 11.5 | 6.4 |

Table A.6 Binder input (DSR results) for MS1–5 days

| | | Binder G* | Phase Angle | Binder G* |
|---|---|---|---|---|
| Temp (°C) | Temp (°F) | (kPa) | (degrees) | (Pa) |
| | | | Binder DSR Test | |
| 76 | 168.8 | 5.44 | 81.4 | 5,440 |
| 82 | 179.6 | 2.64 | 83.7 | 2,640 |
| 88 | 190.4 | 1.32 | 85.7 | 1,320 |

Table A.7 Dynamic modulus inputs for MS1–5 days

| | | Mix Dynamic Modulus (psi) | | |
|---|---|---|---|---|
| Temp (°C) | Temp (°F) | 0.1 Hz | 1 Hz | 10 Hz |
| -10 | 14 | 2,827,249 | 3,259,956 | 3,665,322 |
| 4 | 39.2 | 1,661,109 | 2,144,289 | 2,608,198 |
| 20 | 68 | 540,267 | 956,789 | 1,441,780 |
| 40 | 104 | 71,329 | 175,896 | 392,646 |
| 55 | 131 | 18,640 | 48,583 | 122,857 |

Table A.8 Percent passing in different sieve sizes for MS1–5 days

| Sieve Size | % Passing |
|---|---|
| 3/4 | 100 |
| 3/8 | 94.8 |
| No. 4 | 66.9 |
| No. 200 | 5.6 |

**MS1-12 Days Inputs for Pavement ME:**

Table A.9 Mixture inputs for MS1–12 days

| Binder | | NAMS | $P_{be}$ (weight) | $G_{mb}$ | $P_{be}$ (volume) | $P_b$ (%) |
|---|---|---|---|---|---|---|
| MS1-12 Days | PG 64-22 | 9.5 | 4.9 | 2.332 | 11.4 | 6.4 |

Table A.10 Binder inputs (DSR results) for MS1–12 days

| | | Binder G* | Phase Angle | Binder G* |
|---|---|---|---|---|
| Temp (°C) | Temp (°F) | (kPa) | (degrees) | (Pa) |
| | | | Binder DSR Test | |
| 76 | 168.8 | 9.13 | 78.5 | 9,130 |
| 82 | 179.6 | 4.37 | 81.2 | 4,370 |
| 88 | 190.4 | 2.16 | 83.5 | 2,160 |

Table A.11 Dynamic modulus inputs for MS1–12 days

| Mix Dynamic Modulus (psi) | | | | |
|---|---|---|---|---|
| Temp (°C) | Temp (°F) | 0.1 Hz | 1 Hz | 10 Hz |
| -10 | 14 | 3,028,032 | 3,446,388 | 3,835,125 |
| 4 | 39.2 | 1,843,268 | 2,305,955 | 2,755,725 |
| 20 | 68 | 685,890 | 1,110,027 | 1,576,006 |
| 40 | 104 | 103,311 | 237,644 | 487,543 |
| 55 | 131 | 27,436 | 68,971 | 164,584 |

Table A.12 Percent passing in different sieve sizes for MS1–12 days

| Sieve Size | % Passing |
|---|---|
| 3/4 | 100 |
| 3/8 | 94.8 |
| No 4 | 66.9 |
| No 200 | 5.6 |

## MS4-Unaged Inputs for Pavement ME:

Table A.13 Mixture inputs for MS4-unaged

| Binder | | NAMS | $P_{be}$ (weight) | $G_{mb}$ | $P_{be}$ (volume) | $P_b$ (%) |
|---|---|---|---|---|---|---|
| MS4-unaged | PG 70-22 | 9.5 | 5.1 | 2.4 | 12.2 | 6.3 |

Table A.14 Binder inputs (DSR results) for MS4-unaged

| Binder DSR Test | | | | |
|---|---|---|---|---|
| Temp (°C) | Temp (°F) | Binder G* (kPa) | Phase Angle (degrees) | Binder G* (Pa) |
| 76 | 168.8 | 4.88 | 81.1 | 4,880 |
| 82 | 179.6 | 2.39 | 83.4 | 2,390 |
| 88 | 190.4 | 1.18 | 85.2 | 1,180 |

Table A.15 Dynamic modulus inputs for MS4-unaged

| Mix Dynamic Modulus (psi) | | | | |
|---|---|---|---|---|
| Temp (°C) | Temp (°F) | 0.1 Hz | 1 Hz | 10 Hz |
| -10 | 14 | 311,6621 | 3,564,464 | 3,968,845 |
| 4 | 39.2 | 1,812,726 | 2,347,123 | 2,852,122 |
| 20 | 68 | 594,760 | 1,043,644 | 1,574,997 |
| 40 | 104 | 95,741 | 225,429 | 480,451 |
| 55 | 131 | 31,722 | 79,184 | 189,232 |

Table A.16 Percent passing in different sieve sizes for MS4-unaged

| Sieve Size | % Passing |
|---|---|
| 3/4 | 100 |
| 3/8 | 95.3 |
| No 4 | 69.7 |
| No 200 | 5.5 |

**MS4-5 Days Inputs for Pavement ME:**

Table A.17 Mixture inputs for MS4-5 days

| Binder | | NAMS | $P_{be}$ (weight) | $G_{mb}$ | $P_{be}$ (volume) | $P_b$ (%) |
|---|---|---|---|---|---|---|
| MS4-5 Days | PG 70-22 | 9.5 | 5.1 | 2.4 | 12.2 | 6.3 |

Table A.18 Binder inputs (DSR results) for MS4–5 days

| Binder DSR Test | | | | |
|---|---|---|---|---|
| Temp (°C) | Temp (°F) | Binder G* (kPa) | Phase Angle (degrees) | Binder G* (Pa) |
| 76 | 168.8 | 8.48 | 79.4 | 8,480 |
| 82 | 179.6 | 3.96 | 82 | 3,960 |
| 88 | 190.4 | 1.94 | 84.5 | 1,940 |

Table A.19 Dynamic modulus inputs for MS4–5 days

| Mix Dynamic Modulus (psi) | | | | |
|---|---|---|---|---|
| Temp (°C) | Temp (°F) | 0.1 Hz | 1 Hz | 10 Hz |
| -10 | 14 | 3,306,047 | 3,741,305 | 4,131,174 |
| 4 | 39.2 | 2,006,899 | 2,523,646 | 3,015,655 |
| 20 | 68 | 740,727 | 1,212,455 | 1,736,464 |
| 40 | 104 | 125,008 | 285,303 | 578,366 |
| 55 | 131 | 39,338 | 97,977 | 229,221 |

Table A.20 Percent passing in different sieve sizes for MS4–5 days

| Sieve Size | % Passing |
|---|---|
| 3/4 | 100 |
| 3/8 | 95.3 |
| No 4 | 69.7 |
| No 200 | 5.5 |

**MS4-12 Days Inputs for Pavement ME:**

Table A.21 Mixture inputs for MS4–12 days

| Binder | | NAMS | P$_{be}$ (weight) | G$_{mb}$ | P$_{be}$ (volume) | P$_b$ (%) |
|---|---|---|---|---|---|---|
| MS4-12 Days | PG 70-22 | 9.5 | 5.1 | 2.4 | 12.2 | 6.3 |

Table A.22 Binder inputs (DSR results) for MS4–12 days

| Binder DSR Test | | | | |
|---|---|---|---|---|
| Temp (°C) | Temp (°F) | Binder G* (kPa) | Phase Angle (degrees) | Binder G* (Pa) |
| 76 | 168.8 | 13.7 | 76.5 | 13,700 |
| 82 | 179.6 | 6.52 | 79.5 | 6,520 |
| 88 | 190.4 | 3.15 | 88 | 3,150 |

Table A.23 Dynamic modulus inputs for MS4–12 days

| Mix Dynamic Modulus (psi) | | | | |
|---|---|---|---|---|
| Temp (°C) | Temp (°F) | 0.1 Hz | 1 Hz | 10 Hz |
| -10 | 14 | 4,008,242 | 4,520,788 | 4,913,921 |
| 4 | 39.2 | 2,285,745 | 3,019,087 | 3,694,653 |
| 20 | 68 | 710,440 | 1,276,775 | 1,972,789 |
| 40 | 104 | 97,621 | 249,145 | 558,383 |
| 55 | 131 | 26,842 | 75,476 | 197,656 |

Table A.24 Percent passing in different sieve sizes for MS4–12 days

| Sieve Size | % Passing |
|---|---|
| 3/4 | 100 |
| 3/8 | 95.3 |
| No 4 | 69.7 |
| No 200 | 5.5 |

**RR1-Unaged Inputs for Pavement ME:**

Table A.25 Mixture inputs for RR1-unaged

| Binder | | NAMS | P$_{be}$ (weight) | G$_{mb}$ | P$_{be}$ (volume) | P$_b$ (%) |
|---|---|---|---|---|---|---|
| RR1-Unaged | PG 64-22 | 12.5 | 4.6 | 2.36 | 10.9 | 6.3 |

Table A.26 Binder inputs (DSR results) for RR1-unaged

| | | Binder DSR Test | | |
|---|---|---|---|---|
| Temp (°C) | Temp (°F) | Binder G* (kPa) | Phase Angle (degrees) | Binder G* (Pa) |
| 64 | 147.2 | 8.86 | 78.9 | 8,860 |
| 70 | 158 | 3.94 | 81.7 | 3,940 |
| 76 | 168.8 | 1.84 | 84 | 1,840 |

Table A.27 Dynamic modulus inputs for RR1-unaged

| | | Mix Dynamic Modulus (psi) | | |
|---|---|---|---|---|
| Temp (°C) | Temp (°F) | 0.1 Hz | 1 Hz | 10 Hz |
| -10 | 14 | 2,470,808 | 3,004,417 | 3,508,515 |
| 4 | 39.2 | 1,187,084 | 1,722,696 | 2,271,201 |
| 20 | 68 | 278,143 | 583,538 | 1,028,657 |
| 40 | 104 | 32,202 | 86,280 | 215,542 |
| 55 | 131 | 8,738 | 23,842 | 64,602 |

Table A.28 Percent passing in different sieve sizes for RR1-unaged

| Sieve Size | % Passing |
|---|---|
| 3/4 | 100 |
| 3/8 | 84.3 |
| No 4 | 63 |
| No 200 | 4.9 |

**RR1-5 Days Inputs for Pavement ME:**

Table A.29 Mixture inputs for RR1–5 days

| Binder | | NAMS | $P_{be}$ (weight) | $G_{mb}$ | $P_{be}$ (volume) | $P_b$ (%) |
|---|---|---|---|---|---|---|
| RR1-5 Days | PG 64-22 | 12.5 | 4.6 | 2.363 | 10.9 | 6.3 |

Table A.30 Binder inputs (DSR results) for RR1–5 days

| | | Binder DSR Test | | |
|---|---|---|---|---|
| Temp (°C) | Temp (°F) | Binder G* (kPa) | Phase Angle (degrees) | Binder G* (Pa) |
| 70 | 158 | 6.29 | 80.7 | 6,290 |
| 76 | 168.8 | 2.89 | 83.1 | 2,890 |
| 82 | 179.6 | 1.4 | 85.2 | 1,400 |

Table A.31 Dynamic modulus inputs for RR1–5 days

| Mix Dynamic Modulus (psi) | | | | |
|---|---|---|---|---|
| Temp (°C) | Temp (°F) | 0.1 Hz | 1 Hz | 10 Hz |
| -10 | 14 | 2,676,535 | 3,152,884 | 3,599,767 |
| 4 | 39.2 | 1,400,392 | 1,910,648 | 2,414,764 |
| 20 | 68 | 374,291 | 722,297 | 1,182,375 |
| 40 | 104 | 48,470 | 122,218 | 284,795 |
| 55 | 131 | 14,432 | 37,567 | 95,936 |

Table A.32 Percent passing in different sieve sizes for RR1–5 days

| Sieve Size | % Passing |
|---|---|
| 3/4 | 100 |
| 3/8 | 84.3 |
| No 4 | 63 |
| No 200 | 4.9 |

**RR1-12 Days Inputs for Pavement ME:**

Table A.33 Mixture inputs for RR1–12 days

| Binder | | NAMS | $P_{be}$ (weight) | $G_{mb}$ | $P_{be}$ (volume) | $P_b$ (%) |
|---|---|---|---|---|---|---|
| RR1-12 Days | PG 64-22 | 12.5 | 4.6 | 2.36 | 10.9 | 6.3 |

Table A.34 Binder inputs (DSR results) for RR1–12 days

| Binder DSR Test | | | | |
|---|---|---|---|---|
| Temp (°C) | Temp (°F) | Binder G* (kPa) | Phase Angle (degrees) | Binder G* (Pa) |
| 70 | 158 | 9.74 | 77.8 | 9,740 |
| 76 | 168.8 | 4.44 | 80.8 | 4,440 |
| 82 | 179.6 | 2.1 | 83.3 | 2,100 |

Table A.35 Dynamic modulus inputs for RR1–12 days

| Mix Dynamic Modulus (psi) | | | | |
|---|---|---|---|---|
| Temp (°C) | Temp (°F) | 0.1 Hz | 1 Hz | 10 Hz |
| -10 | 14 | 2,798,899 | 3,247,683 | 3,667,942 |
| 4 | 39.2 | 1,547,583 | 2,031,789 | 2,508,736 |
| 20 | 68 | 477,235 | 845,522 | 1,297,758 |
| 40 | 104 | 69,990 | 164,958 | 355,473 |
| 55 | 131 | 21,410 | 53,351 | 128,104 |

Table A.36 Percent passing in different sieve sizes for RR1–12 days

| Sieve Size | % Passing |
|---|---|
| 3/4 | 100 |
| 3/8 | 84.3 |
| No 4 | 63 |
| No 200 | 4.9 |

**EB4-Unaged Inputs for Pavement ME:**

Table A.37 Mixture input for EB4-unaged

| Binder | | NAMS | $P_{be}$ (weight) | $G_{mb}$ | $P_{be}$ (volume) | $P_b$ (%) |
|---|---|---|---|---|---|---|
| EB4-Unaged | PG 76-22 | 9.5 | 5.2 | 2.319 | 12.1 | 6.7 |

Table A.38 Binder inputs (DSR results) for EB4-unaged

| Binder DSR Test | | | | |
|---|---|---|---|---|
| Temp (°C) | Temp (°F) | Binder G* (kPa) | Phase Angle (degrees) | Binder G* (Pa) |
| 76 | 168.8 | 4.19 | 80 | 4,190 |
| 82 | 179.6 | 2.27 | 82.8 | 2,270 |
| 88 | 190.4 | 1.25 | 84.8 | 1,250 |

Table A.39 Dynamic modulus inputs for EB4-unaged

| Mix Dynamic Modulus (psi) | | | | |
|---|---|---|---|---|
| Temp (°C) | Temp (°F) | 0.1 Hz | 1 Hz | 10 Hz |
| -10 | 14 | 2,658,391 | 3,067,082 | 3,444,938 |
| 4 | 39.2 | 1,524,279 | 2,015,375 | 2,473,954 |
| 20 | 68 | 473,378 | 849,634 | 1,323,620 |
| 40 | 104 | 73,871 | 165,583 | 350,080 |
| 55 | 131 | 23,183 | 52,000 | 117,821 |

Table A.40 Percent passing in different sieve sizes for EB4-unaged

| Sieve Size | % Passing |
|---|---|
| 3/4 | 100 |
| 3/8 | 96.3 |
| No 4 | 72.4 |
| No 200 | 6.7 |

**EB4-5 Days Inputs for Pavement ME:**

Table A.41 Mixture inputs for EB4–5 days

| Binder | | NAMS | P$_{be}$ (weight) | G$_{mb}$ | P$_{be}$ (volume) | P$_b$ (%) |
|---|---|---|---|---|---|---|
| EB4-5 Days | PG 76-22 | 9.5 | 5.2 | 2.319 | 12.1 | 6.7 |

Table A.42 Binder inputs (DSR results) for EB4–5 days

| Binder DSR Test | | | | |
|---|---|---|---|---|
| Temp (°C) | Temp (°F) | Binder G* (kPa) | Phase Angle (degrees) | Binder G* (Pa) |
| 76 | 168.8 | 6.44 | 82.5 | 6,440 |
| 82 | 179.6 | 3.98 | 83.7 | 3,980 |
| 88 | 190.4 | 2 | 84.9 | 2,000 |

Table A.43 Dynamic modulus inputs for EB4–5 days

| Mix Dynamic Modulus (psi) | | | | |
|---|---|---|---|---|
| Temp (°C) | Temp (°F) | 0.1 Hz | 1 Hz | 10 Hz |
| -10 | 14 | 2,715,570 | 3,106,057 | 3,468,665 |
| 4 | 39.2 | 1,642,934 | 2,109,202 | 2,543,839 |
| 20 | 68 | 578,377 | 976,047 | 1,444,726 |
| 40 | 104 | 98,399 | 212,212 | 426,538 |
| 55 | 131 | 30,197 | 66,873 | 146,981 |

Table A.44 Percent passing in different sieve sizes for EB4–5 days

| Sieve Size | % Passing |
|---|---|
| 3/4 | 100 |
| 3/8 | 96.3 |
| No 4 | 72.4 |
| No 200 | 6.7 |

**EB4-12 Days Inputs for Pavement ME:**

Table A.45 Mixture inputs for EB4–12 days

| Binder | | NAMS | P$_{be}$ (weight) | G$_{mb}$ | P$_{be}$ (volume) | P$_b$ (%) |
|---|---|---|---|---|---|---|
| EB4-12 Days | PG 76-22 | 9.5 | 5.2 | 2.319 | 12.1 | 6.7 |

Table A.46 Binder inputs (DSR results) for EB4–12 days

| Binder DSR Test | | | | |
|---|---|---|---|---|
| Temp (℃) | Temp (℉) | Binder G* (kPa) | Phase Angle (degrees) | Binder G* (Pa) |
| 76 | 168.8 | 10.76 | 82.4 | 10,760 |
| 82 | 179.6 | 5.98 | 84.2 | 5,980 |
| 88 | 190.4 | 3.01 | 84.9 | 3,010 |

Table A.47 Dynamic modulus inputs for EB4–12 days

| Mix Dynamic Modulus (psi) | | | | |
|---|---|---|---|---|
| Temp (℃) | Temp (℉) | 0.1 Hz | 1 Hz | 10 Hz |
| -10 | 14 | 2,736,684 | 3,118,731 | 3,472,358 |
| 4 | 39.2 | 1,728,651 | 2,183,634 | 2,607,213 |
| 20 | 68 | 676,112 | 1085,126 | 1,549,399 |
| 40 | 104 | 124,987 | 256,477 | 489,752 |
| 55 | 131 | 36,623 | 77,957 | 164,191 |

Table A.48 Percent passing in different sieve sizes for EB4–12 days

| Sieve Size | % Passing |
|---|---|
| 3/4 | 100 |
| 3/8 | 96.3 |
| No 4 | 72.4 |
| No 200 | 6.7 |

**MS2-Unaged Inputs for Pavement ME:**

Table A.49 Mixture inputs for MS2-unaged

| Binder | | NAMS | $P_{be}$ (weight) | $G_{mb}$ | $P_{be}$ (volume) | $P_b$ (%) |
|---|---|---|---|---|---|---|
| MS2-Unaged | PG 64-22 | 19 | 4 | 2.453 | 9.8 | 5.1 |

Table A.50 Binder inputs (DSR results) for MS2-unaged

| Binder DSR Test | | | | |
|---|---|---|---|---|
| Temp (°C) | Temp (°F) | Binder G* (kPa) | Phase Angle (degrees) | Binder G* (Pa) |
| 64 | 147.2 | 7.47 | 79.7 | 7,470 |
| 70 | 158 | 3.35 | 82.4 | 3,350 |
| 76 | 168.8 | 1.56 | 84.6 | 1,560 |

Table A.51 Dynamic modulus inputs for MS2-unaged

| Mix Dynamic Modulus (psi) | | | | |
|---|---|---|---|---|
| Temp (°C) | Temp (°F) | 0.1 Hz | 1 Hz | 10 Hz |
| -10 | 14 | 4,399,898 | 4,906,117 | 4,989,307 |
| 4 | 39.2 | 2,398,127 | 3,292,148 | 4,074,477 |
| 20 | 68 | 641,308 | 1,230,881 | 2,038,260 |
| 40 | 104 | 37,705 | 99,722 | 248,251 |
| 55 | 131 | 26,302 | 70,303 | 179,807 |

Table A.52 Percent passing in different sieve sizes for MS2-unaged

| Sieve Size | % Passing |
|---|---|
| 3/4 | 95.7 |
| 3/8 | 64.5 |
| No 4 | 39.4 |
| No 200 | 4.9 |

**SP 4-Unaged Inputs for Pavement ME:**

Table A.53 Mixture inputs for SP 4-unaged

| Binder | | NAMS | $P_{be}$ (weight) | $G_{mb}$ | $P_{be}$ (volume) | $P_b$ (%) |
|---|---|---|---|---|---|---|
| SP 4-Unaged | PG 64-22 | 9.5 | 4.9 | 2.321 | 11.4 | 6.1 |

Table A.54 Binder inputs (DSR results) for SP 4-unaged

| Binder DSR Test | | | | |
|---|---|---|---|---|
| Temp (℃) | Temp (℉) | Binder G* (kPa) | Phase Angle (degrees) | Binder G* (Pa) |
| 70 | 158 | 7.82 | 79 | 7,820 |
| 76 | 168.8 | 3.51 | 81.9 | 3,510 |
| 82 | 179.6 | 1.64 | 84.3 | 1,640 |

Table A.55 Dynamic modulus inputs for SP 4-unaged

| Mix Dynamic Modulus (psi) | | | | |
|---|---|---|---|---|
| Temp (℃) | Temp (℉) | 0.1 Hz | 1 Hz | 10 Hz |
| -10 | 14 | 2,451,713 | 2,922,226 | 3,377,838 |
| 4 | 39.2 | 1,266,999 | 1,725,823 | 2,196,184 |
| 20 | 68 | 354,479 | 665,372 | 1,068,749 |
| 40 | 104 | 46,870 | 117,037 | 267,475 |
| 55 | 131 | 13,574 | 35,575 | 90,339 |

Table A.56 Percent passing in different sieve sizes for SP 4-unaged

| Sieve Size | % Passing |
|---|---|
| 3/4 | 100 |
| 3/8 | 96.9 |
| No 4 | 73.6 |
| No 200 | 5.4 |

**SP 4-5 days Inputs for Pavement ME:**

Table A.57 Mixture inputs for SP 4-5 days

| Binder | | NAMS | $P_{be}$ (weight) | $G_{mb}$ | $P_{be}$ (volume) | $P_b$ (%) |
|---|---|---|---|---|---|---|
| SP 4-5 Days | PG 64-22 | 9.5 | 4.9 | 2.33 | 11.4 | 6.1 |

Table A.58 Binder inputs (DSR results) for SP 4–5 days

| Binder DSR Test | | | | |
|---|---|---|---|---|
| Temp (℃) | Temp (℉) | Binder G* (kPa) | Phase Angle (degrees) | Binder G* (Pa) |
| 70 | 158 | 10.9 | 80.4 | 10,900 |
| 76 | 168.8 | 4.97 | 83.5 | 4,970 |
| 82 | 179.6 | 2.33 | 85 | 2,330 |

Table A.59 Dynamic modulus inputs for SP 4–5 days

| | | Mix Dynamic Modulus (psi) | | |
|---|---|---|---|---|
| Temp (°C) | Temp (°F) | 0.1 Hz | 1 Hz | 10 Hz |
| -10 | 14 | 2,453,728 | 2,896,702 | 3,322,716 |
| 4 | 39.2 | 1,296,063 | 1,755,951 | 2,213,582 |
| 20 | 68 | 367,242 | 687,658 | 1,103,774 |
| 40 | 104 | 53,273 | 128,951 | 288,372 |
| 55 | 131 | 17,085 | 42,845 | 104,953 |

Table A.60 Percent passing in different sieve sizes for SP 4–5 days

| Sieve Size | % Passing |
|---|---|
| 3/4 | 100 |
| 3/8 | 96.9 |
| No 4 | 73.6 |
| No 200 | 5.4 |

## SP 4-12 Days Inputs for Pavement ME:

Table A.61 Mixture inputs for SP 4–12 days

| Binder | | NAMS | $P_{be}$ (weight) | $G_{mb}$ | $P_{be}$ (volume) | $P_b$ (%) |
|---|---|---|---|---|---|---|
| SP 4-12 Days | PG 64-22 | 9.5 | 4.9 | 2.327 | 11.4 | 6.1 |

Table A.62 Binder inputs (DSR results) for SP 4–12 days

| | | Binder DSR Test | | |
|---|---|---|---|---|
| Temp (°C) | Temp (°F) | Binder G* (kPa) | Phase Angle (degrees) | Binder G* (Pa) |
| 70 | 158 | 17.65 | 73.2 | 17,650 |
| 76 | 168.8 | 8.06 | 76.6 | 8,060 |
| 82 | 179.6 | 3.73 | 79.9 | 3,730 |

Table A.63 Dynamic modulus inputs for SP 4–12 days

| | | Mix Dynamic Modulus (psi) | | |
|---|---|---|---|---|
| Temp (°C) | Temp (°F) | 0.1 Hz | 1 Hz | 10 Hz |
| -10 | 14 | 2,798,915 | 3,165,855 | 3,512,350 |
| 4 | 39.2 | 1,698,506 | 2,114,661 | 2,513,713 |
| 20 | 68 | 631,053 | 996,913 | 1,412,335 |
| 40 | 104 | 114,426 | 233,410 | 441,142 |
| 55 | 131 | 37,042 | 79,838 | 167,008 |

Table A.64 Percent passing in different sieve sizes for SP 4–12 days

| Sieve Size | % Passing |
|------------|-----------|
| 3/4 | 100 |
| 3/8 | 96.9 |
| No 4 | 73.6 |
| No 200 | 5.4 |

## About the Joint Transportation Research Program (JTRP)

On March 11, 1937, the Indiana Legislature passed an act which authorized the Indiana State Highway Commission to cooperate with and assist Purdue University in developing the best methods of improving and maintaining the highways of the state and the respective counties thereof. That collaborative effort was called the Joint Highway Research Project (JHRP). In 1997 the collaborative venture was renamed as the Joint Transportation Research Program (JTRP) to reflect the state and national efforts to integrate the management and operation of various transportation modes.

The first studies of JHRP were concerned with Test Road No. 1—evaluation of the weathering characteristics of stabilized materials. After World War II, the JHRP program grew substantially and was regularly producing technical reports. Over 1,600 technical reports are now available, published as part of the JHRP and subsequently JTRP collaborative venture between Purdue University and what is now the Indiana Department of Transportation.

Free online access to all reports is provided through a unique collaboration between JTRP and Purdue Libraries. These are available at http://docs.lib.purdue.edu/jtrp.

Further information about JTRP and its current research program is available at http://www.purdue.edu/jtrp.

## About This Report

An open access version of this publication is available online. See the URL in the citation below.

Cho, S., Bagchi, T., Jeon, J., & Haddock, J. E. (2024). *Material characterization and determination of MEPDG input parameters for Indiana Superpave 5 asphalt mixtures* (Joint Transportation Research Program Publication No. FHWA/IN/JTRP-2024/06). West Lafayette, IN: Purdue University. https://doi.org/10.5703/1288284317725